https://doi.org/10.5194/egusphere-2026-4300
Preprint. Discussion started: 24 August 2026

Phytoplankton community responses to 20th century eutrophication of Swiss Plateau lakes: a proxy comparison from short sediment cores

Antonia Klatt[1], Jan Waelchli[1], Daniel B. Nelson[1], Theresa Wietelmann[1], Nathalie Dubois[2,3], S. Nemiah Ladd[1,3]

[1]Department of Environmental Sciences, University of Basel, Bernoullistrasse 32, 4056 Basel, Switzerland
[2]Department of Surface Waters – Research and Management, Eawag, Ueberlandstrasse 133, 8600 Dübendorf, Switzerland
[3]Department of Earth and Planetary Sciences, ETH Zurich, Sonneggstrasse 5, 8092 Zurich, Switzerland

Correspondence to: Antonia Klatt (antonia.klatt@unibas.ch), S. Nemiah Ladd (n.ladd@unibas.ch)

Abstract. During the last century, temperate lakes have been strongly impacted by human eutrophication and climate change, causing shifts in phytoplankton communities and higher abundance of cyanobacteria. Paleolimnological reconstructions can extend the timeframe of observations beyond the extent of monitoring data and reveal long-term changes in aquatic communities. Existing paleolimnological studies often rely on proxies that are solely indicative of individual algal groups. As a result, reconstructing the overall algal community composition remains challenging. Here, we analyzed and cross-validated multiple proxies for phytoplankton community composition in sediment cores from three lakes on the Swiss Plateau that underwent extreme eutrophication in the 20th century. We measured the relative abundance of phytosterols and phytol (phytol:sterol index, PSI) and hydrogen isotope offsets between C16:0 fatty acid and phytol ($\delta^2H_{C16:0\ Acid/Phytol}$) and used these to detect past changes in the relative proportions of eukaryotic algae and cyanobacteria. We compared these new organic geochemical proxies with observational data and with gene amplicon sequence variants (ASVs) from plastid-derived 23S rRNA. PSI and $\delta^2H_{C16:0\ Acid/Phytol}$ values were generally in good agreement with cyanobacterial 23S rRNA ASVs, and all proxies indicated increasing proportions of cyanobacteria in response to eutrophication. However, our study also revealed potential biases associated with each individual algal proxy. Specifically, $\delta^2H_{C16:0\ Acid/Phytol}$ values were impacted by non-algal lipid sources, while the abundance of small coccoid cyanobacterial taxa was overestimated by 23S rRNA ASVs relative to their biovolume. Still, the combination of PSI and $\delta^2H_{C16:0\ Acid/Phytol}$ values with other algal proxies is a promising tool for tracing the long-term relative abundance of cyanobacteria and could provide a comprehensive picture of changes in phytoplankton communities over millennial timescales.

1 Introduction

During the last century, human activities have strongly perturbed many temperate lakes, and the interplay between eutrophication and climate change has often dramatically increased algal productivity and shifted phytoplankton community composition, including more frequent cyanobacterial blooms (e.g., Lotter 1989; Hollander et al., 1992; Naeher et al., 2012;

https://doi.org/10.5194/egusphere-2026-4300
Preprint. Discussion started: 24 August 2026

Naeher et al., 2016; Huisman et al., 2018; Lin et al., 2021; King et al., 2024; X. Yan et al., 2024; Nürnberg 2025). Changes in the proportions of cyanobacteria and eukaryotic algae could affect lake carbon sequestration efficiency, negatively impact water quality, and reduce the nutritional quality available to higher trophic levels of aquatic ecosystems (Tortell, 2000; Huisman et al., 2018; Shen et al., 2018; Hedberg et al., 2021; Deng et al., 2024). To predict future changes in algal communities, model approaches often incorporate results from culturing and observational studies (e.g., Elliott et al., 2005; Arhonditsis et al., 2006; Mieleitner and Reichert, 2008). However, monitoring data often do not extend to timescales before the last century, and while cyanobacterial blooms have increased on a global scale since the Industrial Revolution (Taranu et al., 2015; Huisman et al., 2018), records of long-term fluctuations, especially regarding the abundance of cyanobacteria relative to eukaryotic algae, are often scarce. Paleolimnological approaches can extend observational periods and provide important information about long-term climate- and nutrient-driven shifts in the relative abundance of different types of algae (e.g., Lotter, 1988; Cvetkoska et al., 2021).

Reconstructions of past phytoplankton communities often rely on quantifying diatom frustules or dinoflagellate cysts in sediment records (e.g., Dale and Fjellså, 1994; Lotter, 2001; Hinder et al., 2021; Cvetkoska et al., 2021), but only a limited number of taxa produce physical remains that can be preserved and analyzed from sediments. Other paleolimnological studies measure sedimentary algal pigments (e.g., Makri et al., 2019; Schouten et al., 2025), however, pigments can be prone to rapid degradation (Steenbergen et al., 1994; Reuss et al., 2005).

In contrast, various algal membrane lipids are well preserved in sediments and rocks, and lipid distributions have been used to trace different phytoplankton groups over geologic time (e.g., Schubert et al., 1998; Brocks et al., 2017; Weber et al., 2020). These lipids comprise saturated and unsaturated C_{14} to C_{18} fatty acids, which are synthesized by all phytoplankton groups (Killops and Killops, 2004; Rustan and Drevon, 2005; Taipale et al., 2013) and phytosterols, which reflect different eukaryotic algal groups but are absent in cyanobacteria (Volkman 2003; Killops and Killops, 2004; Martin-Creuzburg et al., 2008; Taipale et al., 2016; Peltomaa et al., 2023). Phytol ((2E,7R,11R)-3,7,11,15-tetramethyl-2-hexadecen-1-ol), the side chain of chlorophyll, is an additional biomarker for all phototrophic organisms (e.g., Killops and Killops, 2004; Witkowski et al., 2020). Besides sedimentary lipid distributions, lipid hydrogen isotope ratios, i.e., δ^2H_{Lipid} values ($\delta^2H = (^2H/^1H)_{sample}/(^2H/^1H)_{VSMOW} - 1$), have the potential to serve as another algal lipid proxy (Klatt et al., 2025; Ladd et al., 2025). Hydrogen isotope fractionation between lipids and biosynthetic source water ($\alpha^2_{Lipid/Water} = (^2H/^1H_{Lipid})/(^2H/^1H_{Water})$) varies among taxonomic groups, leading to significant differences in δ^2H_{Lipid} values among different algal groups growing in the same water (Schouten et al., 2006; Zhang and Sachs, 2007; M'Boule et al., 2014; Heinzelmann et al., 2015; Pilecky et al., 2024; Ladd et al., 2025).

While most algal proxies are indicative of specific algal groups, the ratio between phytol and phytosterols, i.e., the phytol:sterol index (PSI) and the relative offset between δ^2H values of C16:0 fatty acid and phytol ($\delta^2H_{C16:0\ Acid/Phytol} = (\delta^2H_{C16:0\ Acid} +1)/(\delta^2H_{Phytol} +1) - 1$) have been proposed as new proxies to trace shifts in the overall algal community composition (Klatt et al., 2025; Ladd et al., 2025). A study of algal biomass samples collected over the course of one year in a lake water column demonstrated that a high PSI can indicate increased cyanobacteria due to the lack of

https://doi.org/10.5194/egusphere-2026-4300
Preprint. Discussion started: 24 August 2026

phytosterols in this prokaryotic algal group (Klatt et al., 2025). Culturing and mesocosm experiments further revealed that high $\delta^2H_{C16:0\ Acid/Phytol}$ values (> 250 ‰) reflect high relative proportions of cyanobacteria (Ladd et al., 2025). Additionally, high $\delta^2H_{C16:0\ Acid/Phytol}$ values can be due to relative abundances of green algae (Ladd et al., 2025). However, uncertainties remain about the reliability of the new lipid proxies in sediment records. For instance, different degradation susceptibilities among algal lipids associated with lipid ^2H-enrichment and changes in relative abundances, as well as the synthesis of fatty acids by bacteria living in sediments, could complicate the interpretation of sedimentary PSI and $\delta^2H_{C16:0\ Acid/Phytol}$ values (Kawamura et al., 1987; Gray et al., 2002; Sachs and Schwab, 2011; Ladd et al., 2018).

In addition to sedimentary lipids, sedimentary DNA (*sed*DNA) - specifically, the analysis of phytoplankton amplicon sequence variants (ASVs) - is another promising proxy to reconstruct algal community dynamics in the past. For instance, a primer set targeting cyanobacterial and eukaryotic algal plastid 23S rRNA genes has been successfully applied to trace past changes in relative abundances of different groups of algae (Sherwood and Presting, 2007; Steven et al., 2012; Hou et al., 2014; Yan et al., 2023; King et al., 2024; D. Yan et al., 2024). Nevertheless, DNA preservation is generally poor for timescales exceeding the early Holocene, and the reflection of past algal communities can be biased by preferential DNA diagenesis (e.g., Boere et al., 2011; Capo et al., 2015; Nwosu et al., 2023; Thorpe et al., 2024).

In this study, we compared sedimentary alcohol distributions, PSI and $\delta^2H_{C16:0\ Acid/Phytol}$ values with ASVs of cyanobacterial and eukaryotic algal plastid 23S rRNA genes to trace changes in phytoplankton communities in different Swiss lakes during the 20th century. We collected sediment cores from three lakes (Greifensee, Murtensee, and Zugersee) on the Swiss Plateau, all of which experienced strong eutrophication and partial recovery during the 20th century (Fig. 1) (e.g., Furrer and Gächter, 1972; Hollander et al., 1992; AquaPlus, 2001; Lotter, 2001; AquaPlus, 2004; Makri et al., 2019). In all lakes, the input of nutrients, especially phosphorus, as well as subsequent remediation measures, have led to changes in phytoplankton community composition (Brutschy, 1912; Soracreppa, 1978; Bürgi et al., 2003; Makri et al., 2019). These changes have been partially documented by algal cell counts in the water column, which are, however, limited to single lakes and specific time intervals (Brutschy, 1912; Soracreppa, 1978; Bürgi et al., 2003; Merz et al., 2023). The comparison between PSI, $\delta^2H_{C16:0\ Acid/Phytol}$ values and ASVs, as well as the cross-validation with other algal proxies and available phytoplankton cell counts allows us to assess potential biases of the different algal proxies in the sediment record.

https://doi.org/10.5194/egusphere-2026-4300
Preprint. Discussion started: 24 August 2026

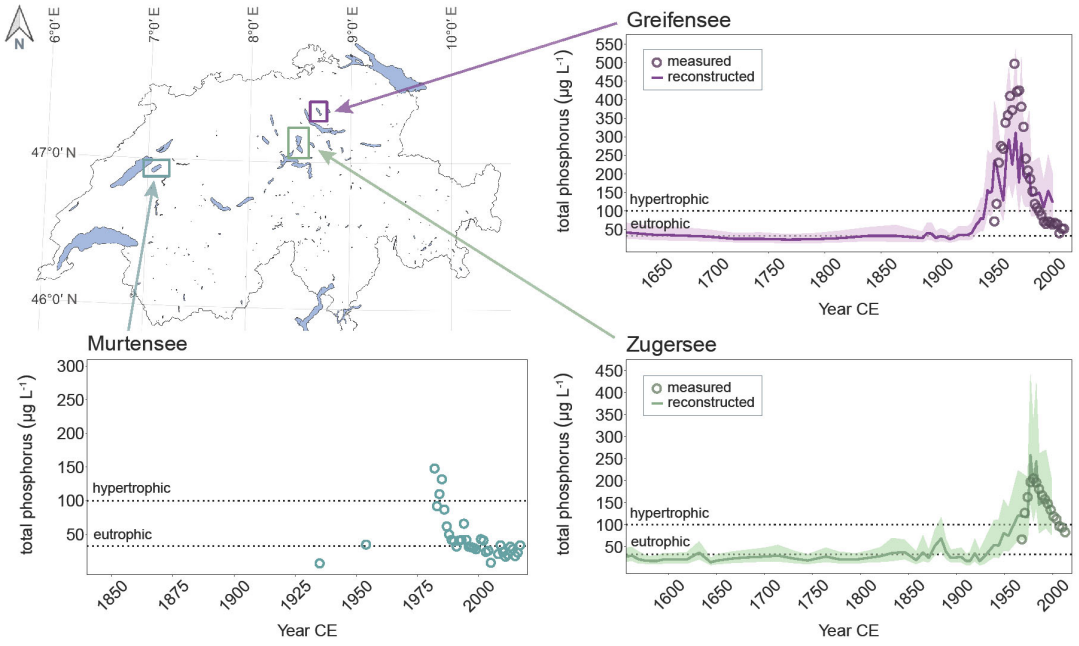

Figure 1: Location and historical changes in Total Phosphorus (TP) concentrations of Greifensee, Murtensee and Zugersee. All lakes are located in the Swiss Plateau. TP concentrations are based on lake water quality monitoring data from the Swiss Federal Office for the Environment and Rivier (1936) (Murtensee). Only a subset of TP measurements is shown for Greifensee and Zugersee for better visualization. In addition to measurement data, reconstructions of TP concentrations based on sedimentary diatom frustules are shown for Greifensee and Zugersee (shaded areas represent the minimum and maximum TP concentrations based on a 2-component weighted-averaging partial least squares model) (AquaPlus, 2001; AquaPlus, 2004). Eutrophic (30-100 µg L^{-1} TP) and hypertrophic conditions (> 100 µg L^{-1} TP) are defined according to Lampert and Sommer (1993). The map of Switzerland with lake locations was accessed from swissBOUNDARIES3D and swissTLM3D (© swisstopo) and plotted with the QGIS Geographic Information System.

2 Material and Methods

2.1 Study site descriptions and core collections

All sediment cores were collected in polycarbonate liners with a UWITEC gravity corer (diameter = 60 mm). All cores were stored vertically at 4 °C prior to subsampling except for the cores from Greifensee collected for lipid extractions (Sect. 2.1.1).

2.1.1 Greifensee

Greifensee is a dimictic, seasonally stratified lake located close to Zurich in the eastern part of the Swiss Plateau at 435 m a.s.l., with a surface area of 8.46 km^2 and a maximum depth of 32 m (Fig. S1a) (Lotter, 2001; Bürgi et al., 2003;

https://doi.org/10.5194/egusphere-2026-4300
Preprint. Discussion started: 24 August 2026

Huntscha et al., 2018). Trophic reconstructions based on diatom frustules indicate that phosphorus concentrations increased strongly in the 1930s to > 60 µg L^{-1}, with the lake reaching hypertrophic conditions ~ 1950 CE (> 100 µg L^{-1} TP; Lampert and Sommer, 1993) (Bürgi et al., 2003; AquaPlus, 2004). Maximum eutrophication occurred from the 1950s to 1970s with measured TP concentrations reaching almost 500 µg L^{-1} (Fig. 1) (AWEL Zurich; FOEN). Due to sewage treatment measures in the catchment area and restrictions regarding P-containing detergents, TP concentrations decreased again in the late 1970s (Bürgi et al., 2003), but Greifensee remains a eutrophic lake presently with slightly higher TP concentrations compared to the 19th century (Bürgi et al., 2003; AquaPlus, 2004; AWEL Zurich; FOEN). Four short sediment cores were collected at the deepest part of the lake (Fig. S1a). The first three cores (all slightly less than 100 cm) (47°21.24' N 8°40.44' E, WSG84) were collected in October 2018 for lipid analysis, while the fourth core (91 cm) (47°20.993' N 8°40.683' E, WSG84) was collected in May 2024 for *sed*DNA analysis. The three cores for lipid analyses were split longitudinally on the day of collection, allowed to oxidize at 4 °C for three days and then subsampled for lipid extractions.

2.1.2 Murtensee

Murtensee is a monomictic seasonally stratified lake located in the western part of the Swiss Plateau at 429 m a.s.l. with a surface area of 22.8 km^2 and a maximum depth of 45 m (Fig. S1b) (Makri et al., 2019). Only limited measurements of TP in the water column are available, but mesotrophic conditions with moderate phosphorus concentrations of ~ 7 µg L^{-1} were described in 1935 (Rivier, 1936). By 1954, TP measurements already reflected eutrophic conditions (> 32.5 µg L^{-1} TP; Lampert and Sommer, 1993) (FOEN; canton Fribourg) (Fig. 1). Due to a lack of measurements in the 1960s and 1970s, the specific timing of maximum eutrophication is unknown, but TP values were measured in 1982 CE (148 µg L^{-1} TP) indicating hypertrophic conditions. Following the construction of wastewater treatment plants and implementation of restrictions on the use of P-containing detergents and agricultural fertilizers, phosphorus concentrations decreased during the 1980s, and Murtensee reached mesotrophic conditions in the 2000s (Makri et al., 2019). A short sediment core (89 cm) was collected in April 2023 at ~ 40 m water depth (46°55.7699' N 7°4.0267' E, WSG84) (Fig. S1b).

2.1.3 Zugersee

Zugersee is located near the city of Zug in the eastern part of the Swiss Plateau at 413 m a.s.l. with a surface area of 38.2 km^2 (Strassmann et al., 2005; Maerki et al., 2009). The lake consists of a northern and a southern basin which are separated by a peninsula within a transition zone (Fig. S2a) (Brutschy, 1912; Dittrich et al., 2009). The shallower northern basin has a maximum water depth of 60 m, and the water column mixes during the spring turnover (Mengis et al., 1997; Dittrich et al., 2009). The southern basin has a maximum water depth of 200 m with steep slopes, and nearly permanent anoxia occurs below 100 m (Dittrich 2009; Maerki et al., 2009). In contrast to the northern basin, the southern basin is wind-sheltered by surrounding mountains (Fig. S2a) (Dittrich et al., 2009). Nutrient releases from the city of Zug into the northern basin already occurred during the early 1900s (Brutschy, 1912). Trophic reconstructions in the southern basin indicate a strong increase in phosphorus concentrations in the late 1930s and the lake reached hypertrophic conditions in the 1960s (AquaPlus,

https://doi.org/10.5194/egusphere-2026-4300
Preprint. Discussion started: 24 August 2026

2001). Maximum eutrophication occurred during the 1970s to 1980s with the highest TP measurements of > 200 µg L^{-1} (FOEN; canton Zug). With the establishment of a wastewater treatment plant and reductions in the use of agricultural fertilizers, TP concentrations decreased in the late 1980s but remained relatively high in the early 2000s (~ 90 µg L^{-1} TP) (AquaPlus, 2001). Two short sediment cores were collected in September 2024 (Fig. S2). The first core (51 cm) was taken in the northern basin (47°9.8075' N 8°28.7821' E, WSG84) at a water depth of 39 m, the second core (43 cm) was collected in the southern basin (47°5.4576' N 8°30.1058' E, WSG84) at a water depth of 197 m (Fig. S2a).

2.2 Dating and age models

The age-depth profile of the two cores from Greifensee were determined by counting varves, which were clearly visible in the sediment record starting from the mid-1930s. For the age determination of additional samples from deeper parts of the core, we assumed sedimentation rates of 5 years cm^{-1} according to Hollander et al. (1992).

The dating of the other cores from Murtensee and Zugersee was based on measurements of ^{210}Pb, ^{226}Ra and ^{137}Cs in 0.5 to 5 g dry sediment samples by gamma spectroscopy on a high-purity WELL™ Germanium Well Detector (Mirion Technologies, Canberra, AU) at the Swiss Federal Institute of Aquatic Science and Technology (Eawag) in Dübendorf. Age-depth models were established by Bayesian statistics using the 'rplum' package (version 1.0.0; Aquino-López et al., 2018) in R (version 4.4.1, R Core Team 2024, Vienna, AT) with BCE/CE as calendar scale (Fig. S3). The dry density of each sample was calculated based on its dry weight and the volume of the wet sample. We assumed constant ^{226}Ra throughout the sediment cores. For the short core from the southern basin of Zugersee, samples from turbidite layers (Fig. S2b) were excluded from the model. Reported sample ages derived from mean ages and sedimentation rates estimated by age depth modeling (Fig. S3). Additional age uncertainties related to ^{210}Pb and ^{137}Cs dating and the modeling approach (Fig. S3) were not included in the results to be consistent with samples from Greifensee.

2.3 Sedimentary DNA extractions

Sediment samples for DNA extractions were collected before the subsampling of lipid samples in a lab that had been thoroughly cleaned with 2 % deconex® (Borer Chemie AG, Zuchwil, CH). The subsampling area was additionally cleaned with DNA-ExitusPlus™ (Huberlab AG, Aesch, CH) and MilliQ water. Subsampling occurred at room temperature under clean conditions, following current best practices modified from Epp et al. (2019). Potential contamination during the subsampling was assessed with air control samples as described by Armbrecht et al. (2022). Samples were taken every third cm from the center of longitudinally split core halves and stored at -20 °C prior to extractions. For Greifensee and Murtensee, extractions were not performed for all samples.

*Sed*DNA was extracted with the DNeasy® PowerLyzer® PowerSoil® Kit for Soil DNA Extraction (Qiagen, Hilden, DE). We followed the manufacturer's instructions with the following adjustments adapted from Epp et al. (2019): non-frozen wet sediment was homogenized with a sterile spatula and ~ 0.5 g of homogenized sediment was added to the PowerBead Tube, samples were mixed for 10 min on a vibratory mixer (highest speed), 20 µl of 2 mg ml^{-1} proteinase K in 5 mM Tris HCl

https://doi.org/10.5194/egusphere-2026-4300
Preprint. Discussion started: 24 August 2026

buffer pH 8 was added, and samples were gently rotated at 56 °C overnight. The extracted DNA was eluted with 100 µl C6 solution and 60 – 100 µl of extracted DNA was further purified with the OneStep™ PCR Inhibitor Removal Kit (Zymo research, Irvine, CA, USA) following the manufacturer's protocol. During all extractions and purifications, sample tubes, spin columns and buffer solutions were only opened under a laminar flow hood. DNA concentrations were determined with a Qubit dsDNA broad range assay kit (Thermo Scientific, Waltham, MA, USA) according to the manufacturer's instructions and 10 ng of DNA in 25 µl C6 solution from each sample was prepared for further processing. DNA extracts were stored at -20 °C.

2.4 Amplicon sequencing and data processing

Library preparation and amplicon sequencing were performed at the Genomics Facility Basel, operated by the University of Basel and the Department of Biosystems Science and Engineering (D-BSSE), ETH Zurich. Library preparation was conducted once per sample using a two-step PCR approach. In the first PCR, published algal specific primers (p23SrV_f1: 5' GGA CAG AAA GAC CCT ATG AA 3' and p23SrV_r1: 5' TCA GCC TGT TAT CCC TAG AG 3') were used to amplify a ~ 400 bp fragment from the domain V of the cyanobacterial and eukaryotic algal plastid 23S rRNA gene (Sheerwood and Presting, 2007). Primers were modified as phased amplicon primers with up to eight nucleotides attached to the beginning of the primer sequence (TableS1, S2) to increase amplicon diversity for accurate sequencing. The first PCR was performed in a 25 µl reaction (KAPA HiFi HotStart) containing 4 µl DNA template, 1 µM primer mix, and 0.5x SYBR Green (Life Technologies) in an iconPCR system (n6) with autonormalisation (3x baseline signal) in 19 to 25 cycles. The thermal cycling parameters were initial denaturation at 98 °C for 2 min, denaturation 15 sec, primer annealing at 55 °C for 20 s, extension at 72 °C for 30 s and a final extension at 72 °C for 2 min. After PCR, reactions were purified with 0.8x SPRI beads (Beckman Coulter Life Sciences, Brea, CA, USA) according to the manufacturer's protocol and eluted in 20 µl H_2O. For the second PCR, Nextera XT UDI primers (Illumina) were used containing the sequencing adapter and an 8/8 bp dual barcode unique for each sample. The reaction (KAPA HiFi HotStart) included 8 µl of the purified PCR product, 2.5 µl IDX primer mix, and 0.5x SYBR Green. PCR was performed with the same thermal parameters as the first PCR in 8 cycles without autonormalisation. After purification with 0.8x SPRI beads, libraries were pooled (5 µl of each sample) and 2x 300 paired end sequencing was performed on an AVITI™ system (Element Biosciences, San Diego, CA, USA). Raw sequencing reads were demultiplexed with Bases2FastQ. For Greifensee, a total of 22,437,721 raw reads were obtained from 17 samples, for Murtensee a total of 17,461,179 raw reads were obtained from 13 samples. 17,896,024 total raw reads were obtained from 14 samples of the northern basin of Zugersee, and 21,309,917 reads were obtained from 14 samples of the southern basin. Three samples from Zugersee yielded no sequencing reads, which included one *sed*DNA sample and a subsampling blank from the northern basin, and an extraction blank from the southern basin.

Primer sequences were trimmed with cutadapt v4.2 (error 0.1, no indels) and raw reads were processed following the workflow described in Gfeller et al. (2023) using the 'dada2' package (version 1.34.0; Callahan et al., 2016) in R (version 4.4.1) for quality filtering, read merging and inferring exact ASVs. We allowed two maximum expected errors for quality

https://doi.org/10.5194/egusphere-2026-4300
Preprint. Discussion started: 24 August 2026

filtering and truncated only reverse sequences at 220 bp. Error rates were based on all samples of the sequencing run, which initially contained 15 additional samples from Lac de Neuchâtel which were not included in this study. Taxonomic assignments of the 23S rRNA ASVs were performed using the Basic Local Alignment Search Tool (BLAST) with the National Center for Biotechnology Information (NCBI) database (accessed on 5th June 2026). These calculations were performed at sciCORE (http://scicore.unibas.ch/), the scientific computing center of the University of Basel. For downstream analysis, samples with a low sequence number (threshold 390,000 sequences) were removed, which comprised all subsampling and extraction blanks. Alignments were filtered for algal classes and non-algal ASVs were not considered for further analysis. Absolute algal ASV counts were normalized by total sum scaling, after confirming no significant differences in sequencing depths between lakes *via* Kruskal-Wallis rank sum test (Weiss et al., 2017). Outlier detection was performed with the CLOUD method (Montassier et al., 2018) based on Bray Curtis distances of normalized ASV data for each lake with nearest neighbours set to 40 % of the sample size and an empirical outlier percentile of 0.1.

2.5 Bulk Total Organic Carbon

Prior to measurements of bulk Total Organic Carbon (TOC) of samples, inorganic carbon was removed from sediment samples by acidification. ~ 10 mg of dry sediment was weighed into silver capsules and two drops of MilliQ water were added to each sample. Then, samples were acidified by the vapor phase of 37 % HCl for 24 h and dried at 40 to 50 °C for at least four days. Samples were then folded into tin capsules and TOC was measured on a Flash 2000 elemental analyzer (EA) equipped with a thermal conductivity detector coupled to a Delta Plus XP IRMS (Thermo Scientific) with a MAS 200R autosampler.

2.6 Lipid extraction and quantification

For lipid extractions from the Murtensee and Zugersee cores, 2 cm of sediment without contact to the polycarbonate liner was subsampled every second cm from the split core halves and stored in combusted glass vials at -20 °C. Total Lipid Extracts (TLEs) of ~ 5 g dry sediment were extracted in 9:1 dichloromethane:methanol (DCM:MeOH) with an accelerated solvent extraction system (Dionex™ ASE™ 350, Thermo Scientific), as described in Hirave et al. (2021). A recovery standard containing a mix of hexatriacontane (*n*-C_{36}-alkane), 2-octadecanone, heneicosanol (*n*-C_{21}-alkanol), and nonadecanoic acid (*n*-C19:0 acid) was quantitatively added to each sample prior to extractions. TLEs were dried in a Rocket Evaporator (Genevac, Ipswich, UK) and base-saponified as in Klatt et al. (2025). Following saponification, the neutral and acid fractions were separated by heptane rinses and subsequent acidification of the aqueous fraction according to Klatt et al. (2025).

Neutral fractions were separated into compound classes using silica gel column chromatography. Fractions were dissolved in 9:1 DCM:MeOH, mixed with ~ 0.14 g of 5 % deactivated silica gel (0.04-0.063 mm (400-230 mesh), Carl Roth, Karlsruhe, DE), and gently dried under nitrogen. The dry mixture was loaded onto a glass cartridge containing ~ 1.4 g of 5 % deactivated silica gel. Hydrocarbons and ketones were eluted in 20 ml heptane and 18 ml 2:1 heptane:DCM. Alcohols

https://doi.org/10.5194/egusphere-2026-4300
Preprint. Discussion started: 24 August 2026

(including phytol and phytosterols) were eluted with 20 ml DCM. For quantification and identification of alcohols, 5 % aliquots were silylated as in Ladd et al. (2025) and analyzed within 48 h. The remaining 95 % of each alcohol fraction was acetylated as in Klatt et al. (2025) and used for δ^2H_{Phytol} measurements. Acid fractions were methylated directly after saponification to form fatty acid methyl-esters (FAMEs) using HCl in MeOH as in Klatt et al. (2025). Saturated FAMEs (including C16:0 FAME) were purified with 10 wt % $AgNO_3$-impregnated silica gel columns (~ 0.5 g) and eluted with 8 ml 1:1 heptane:DCM.

Acetylated alcohols and FAMEs were quantified with gas chromatography–flame ionization detection (GC-FID) as in Baan et al. (2023). For silylated alcohols, the column (Rxi-5ms, 60 m x 25 mm x 25 µm (Restek, Bad Homburg vor der Höhe, Germany)) was held at 60 °C for 2 min, heated to 290 °C at 15 °C min^{-1} and then to 325 °C at 6 °C min^{-1}. The oven was held at its final temperature of 325 °C for 10 min.

To identify different alcohol compounds, mass spectra of a subset of silylated samples were analyzed by gas chromatography-mass spectrometry (GC–MS) on a Trace™ GC Ultra gas chromatograph coupled to a DSQ II mass spectrometer (Thermo Scientific) with a Rxi-5ms column (60 m x 25 mm x 25 µm) (Restek). The column was held at 50 °C for 2 min, heated to 140 °C at 10 °C min^{-1}, held for 1 min, heated to 300 °C at 4 °C min^{-1}, held for 36 min, and heated to a 320 °C at 10 °C min^{-1} and held for 10 min. Mass spectra were compared to published references (National Institute of Standards and Technology; Venkatesan, 1989; Goad and Akihisa, 1997; Elvert and Niemann, 2008; Atwood et al., 2014; Peltomaa et al., 2023) and internal collections. The retention time of an external C16:0 FAME standard (Sulpelco® C_8-C_{24} FAME Mix) (Merck KGaA, Darmstadt, Germany) was used to identify C16:0 FAME in our samples.

For the lipid extractions from Greifensee cores, samples were taken after oxidation of the split core halves in three-year intervals to the bottom of the varved section (24 to 27.5 cm). One of these cores was additionally subsampled in 2 cm intervals from 24 to 44 cm. All lipid samples were stored at -20 °C prior to subsequent analyses. TLEs were extracted in a Microwave Reaction System (SolvPro, Anton Paar, Graz, Austria) according to Ladd et al. (2018). Further lipid processing including saponification, as well as purification of alcohol and acid fractions generally followed the same procedures described for the samples from Murtensee and Zugersee. Detailed descriptions of the methods with instrument specifications were published in Ladd et al. (2018). Alcohol compounds were quantified and identified based on the analysis of silylated 2.5 % aliquots by GC-FID and GC-MS as described for the samples from Murtensee and Zugersee.

Sedimentary alcohol concentrations (µg g^{-1} dry sediment) were calculated based on added amounts of the *n*-C_{21}-alkanol recovery standard and normalized to TOC (% of dry sediment weight). For Greifensee, no TOC measurements were available, and TOC values were estimated based on linear interpolation from published TOC measurements of a core collected in 2014 at a similar location (Chiaia-Hernández et al., 2017).

2.7 Lipid δ^2H measurements

Lipid δ^2H values from Murtensee samples were measured by gas chromatography-isotope ratio mass spectrometry (GC-IRMS, ThermoScientific) at the Stable Isotope Ecology Laboratory at University of Basel, using the same

https://doi.org/10.5194/egusphere-2026-4300
Preprint. Discussion started: 24 August 2026

instrumentation as in Baan et al. (2023). For C16:0 fatty acid, the column (Rtx-5ms, 30 m x 0.25 mm x 0.25 µm (Restek)) was heated from 60 to 140 °C at 15 °C min^{-1}, and from 140 to 325 °C at 4 °C min^{-1}, then kept at 325 °C for 15 min. For phytol, the column was heated from 60 to 140 °C at 15 °C min^{-1}, and from 140 to 320 °C at 6 °C min^{-1}, then kept at 320 °C for 9 min. The column effluent entered a ceramic pyrolysis reactor and was converted to H_2 gas at 1420 °C.

Measured δ^2H values from the Thermo Isodat 3.0 software (Thermo Scientific) were converted to the Vienna Standard Mean Ocean Water (VSMOW) scale and corrected for isotopic effects related to time drift, peak size and retention time using multiple linear regressions between known and measured values of external standards (FAME Mix F8-3 and *n*-alkane Mix A7 from Indiana University and C20:0 FAME USGS71 from the United States Geological Survey. An additional quality control (QC) standard (FAME Mix F8-4, Indiana University) was measured multiple times throughout each sequence and scale-normalized to VSMOW with the same method as the samples. For δ^2H_{Phytol} measurements, a phytol acetate standard (Penta Manufacturing, Livingston, NJ) was included to monitor the relationship between δ^2H values and peak area and to track long-term precision. The average standard deviation (SD) for all QC compounds was 2.8 ‰ with an average offset of 1.8 ‰ from their known values (n = 70). The H_3^+ factor was determined at the beginning of each sequence and averaged 2.7 +/- 0.23 ppm nA^{-1}. δ^2H_{Lipid} values were corrected for hydrogen added during derivatization using isotopic mass balance as in Nelson and Sachs (2014). The δ^2H value of the acetyl group was determined by acetylation of sucrose with a known δ^2H value and the δ^2H value of the methyl group was obtained by methylating phthalic acid with a known δ^2H value (Indiana University). Analytical uncertainties were calculated from replicate measurements and propagated errors from the uncertainties in the δ^2H values of added hydrogen.

Lipid δ^2H values from Greifensee samples were measured at Eawag in Kastanienbaum using instrumentation and methodology as in Ladd et al. (2025). Different *n*-alkanes (*n*-C_{17}, C_{19}, C_{21}, C_{23}, C_{25}, C_{28}, C_{34}) (Indiana University) were used as reference standards to normalize measurements to the VSMOW scale and to correct for isotopic effects associated with retention time, peak size, and analytical drift. A *n*-C_{29} alkane standard, which has been routinely measured in the Stable Isotope Ecology Laboratory at University of Basel, was used as additional QC and analyzed three times throughout each sequence. The average SD was 10 ‰ with an average offset of 1.2 ‰ from its long-term reported δ^2H value (n = 31). The H_3^+ factor averaged 3.6 +/- 0.18 ppm nA^{-1}. The correction of δ^2H_{Phytol} values for hydrogen added by derivatization was based on approximations of δ^2H values of the acetyl group by measuring acetylated and unacetylated *n*-C_{10}-alkanol.

2.8 Calculations and Statistics

All data analyses were carried out in R (R version 4.4.1, R Core Team 2024, Vienna, AT) and RStudio (2023.06.1+524). The 'ggplot2' (Wickham, 2009) and the 'cowplot' package (Wilke, 2025) were used for visualizations.

2.8.1 Phytol:sterol index

PSI values were calculated based on sedimentary concentrations [µg g^{-1} TOC] of phytol and various phytosterols (Eq. (1), (2), and (3)). For each lake, potential terrestrial sources of phytosterols were assessed by non-metric multidimensional

https://doi.org/10.5194/egusphere-2026-4300
Preprint. Discussion started: 24 August 2026

scaling (NMDS) of phytosterols and terrestrial triterpenoids (Fig. S4; see Table S3 for systemic names) and equations were adjusted accordingly.

Phytosterols and stanols included brassicasterol, campesterol, campestanol, stigmasterol, sitosterol, sitostanol, chondrillasterol, 22-dihydrochondrillasterol, dinosterol, 4α-desmethyl-dinosterol, dehydro-dinosterol, dinostanol. Terrestrial triterpenoids included α- and β-amyrin and lupeol. Dinosterol and its derivatives were always included in PSI calculations due to their source-specificity for dinoflagellates (and other eukaryotic algae) (Meyers and Ishiwatari, 1993; Volkman, 2003). For Murtensee, 4α-desmethyl-dinosterol was not detected.

The PSI for Greifensee was calculated by:

$$PSI = \frac{[\text{phytol}]}{\begin{array}{c}([\text{phytol}]+[\text{brassicasterol}]+[\text{campesterol}]+[4\alpha-\text{desmethyl}-\text{dinosterol}]+\\ [\text{dehydro}-\text{dinosterol}]+[\text{dinostanol}]+[\text{dinosterol}]+[\text{sitostanol}]+[\text{sitosterol}])\end{array}} \quad (1)$$

The PSI for Murtensee was calculated by:

$$PSI = \frac{[\text{phytol}]}{\begin{array}{c}([\text{phytol}]+[\text{brassicasterol}]+[\text{campesterol}]+[\text{dehydro}-\text{dinosterol}]+\\ [\text{dinostanol}]+[\text{dinosterol}]+[\text{sitosterol}]+[\text{stigmasterol}])\end{array}} \quad (2)$$

The PSI of Zugersee was calculated by:

$$PSI = \frac{[\text{phytol}]}{\begin{array}{c}([\text{phytol}]+[\text{brassicasterol}]+[\text{campesterol}]+[4\alpha-\text{desmethyl}-\text{dinosterol}]+[\text{dehydro}-\text{dinosterol}]+\\ [\text{dinostanol}]+[\text{dinosterol}]+[\text{sitostanol}]+[\text{sitosterol}]+[\text{stigmasterol}])\end{array}} \quad (3)$$

2.8.2 Phytoplankton biovolume calculation

Phytoplankton biovolume in Greifensee and Murtensee was calculated based on published algal cell counts from Bürgi et al. (2003) and Merz et al. (2023). For Greifensee, cell counts comprised 0 to 20 m water depth and were conducted from 1972 to 2021 CE. For Murtensee, cell counts comprised 0 to 10 m water depth from 1999 to 2011 CE and 0 to 15 m water depth from 2012 to 2022 CE. Cell counts from single algal species were multiplied by biovolume measurements from individual phytoplankton cells (Narwani et al., 2019). In single cases, the species biovolume was unknown and the biovolume reported for the genus ('sp.') or the median of all species from the respective family was used. Afterwards, algal biovolume was summed for each taxonomic class and each sampling year.

2.8.3 Statistical analyses

NMDS of relative alcohol concentrations and ASV abundances was performed with the 'metaMDS' function of the 'vegan' package (Oksanen et al., 2025) based on Bray Curtis distances with k=3 dimensions data were square root transformed if NMDS plots displayed an 'arch' effect (Podani and Miklós, 2002). Relative concentrations were calculated as the contribution of individual compounds to the sum concentration of all compounds.

https://doi.org/10.5194/egusphere-2026-4300
Preprint. Discussion started: 24 August 2026

Locally estimated scatterplot smoothing (LOESS) fits were generated to estimate trends of PSI values and $\delta^2H_{C16:0/Phytol}$ values with the 'loess' function from base R (R Core Team 2024, Vienna, AT). Smoothing span parameters for each model were defined by leave-one-out k-fold cross validation with the 'train' function of the 'caret' package (Kuhn, 2008).

Stratigraphically constrained clustering (CONISS) of relative alcohol and ASV distributions was performed with the 'chchlust' function of the 'rioja' package (Juggins, 2024).

For cluster analysis of alcohols, *n*-alkanols were excluded due to the large variability of possible source organisms (e.g., Zhang et al., 2021). The dissimilarity matrix for cluster analysis was created with the 'vegdist' function of the 'vegan' package (Oksanen et al., 2025) based on Bray Curtis distances. The number of significant clusters was determined with the broken stick model. For plotting, the dendrogram was extracted with the 'dendro_data' function of the 'ggdendro' package (de Vries and Ripley, 2024).

The phylogenetic tree from cyanobacterial and plastid 23S rRNA ASVs was generated with the 'ggtree' package (Yu et al., 2017; Yu et al., 2018; Yu, 2020; Xu et al., 2022), the 'ggtreeExtra' package (Xu et al., 2021) and the 'treeio' package (Wang et al., 2020).

3 Results

To reconstruct how phytoplankton community composition changed in response to eutrophication, we performed hierarchical cluster analysis of sedimentary alcohol distributions and algal 23S rRNA ASVs. We reconstructed the relative proportion of cyanobacteria and eukaryotic algae based on the PSI, $\delta^2H_{C16:0\ Acid/Phytol}$ values and cyanobacterial 23S rRNA ASVs and further examined alterations in the abundances of ASVs of different algal classes. For Zugersee, measurements of δ^2H_{Phytol} values were not possible due to unresolved complex mixtures co-eluting with phytol in the GC-chromatogram (Farrington and Quinn, 2015).

In addition to phytoplankton derived ASVs, amplicons from algal classes comprising mainly macroalgae, i.e., Bangiophyceae and Ulvophyceae, were included in the analysis due to their high relative abundances before hypertrophic conditions and the potential impact on lipid proxies.

3.1 Greifensee

In Greifensee, the PSI was relatively stable from the mid-1800s until ~ 1940, but smaller peaks occurred ~ 1850 CE, from ~ 1870 to 1880 CE, and from ~ 1920 to 1930 CE (Fig. 2a). PSI values strongly increased in 1941-1943 CE, co-occurring with significant changes in sedimentary alcohol distributions. After 1950-1952 CE, the PSI decreased and reached their lowest value in 1971-1973 CE. Afterwards, PSI values slightly increased again but remained rather low, with fluctuating values.

https://doi.org/10.5194/egusphere-2026-4300
Preprint. Discussion started: 24 August 2026

$\delta^2H_{C16:0\ Acid/Phytol}$ values ranged from 251 ‰ in ~ 1910 CE to 316 ‰ in 1992-1994 CE spanning a total range of 65 ‰. (Fig. 2a). $\delta^2H_{C16:0\ Acid/Phytol}$ values were relatively stable from the mid-1800s until ~ 1940 CE with some fluctuations. $\delta^2H_{C16:0\ Acid/Phytol}$ values displayed a strong increase in 1941-1943 CE, again co-occurring with significant changes in alcohol clusters. Subsequently, $\delta^2H_{C16:0\ Acid/Phytol}$ values fluctuated with an overall increasing trend.

The abundance of 23S rRNA ASVs of Cyanobacteriota was relatively stable during the 1800s until ~ 1940 CE, ranging between 18 % and 33 % (Fig. 2a). In the 1940s, the relative abundance of cyanobacterial ASVs strongly increased, reaching 86 % in ~ 1948 CE. After a drop to 21 % in ~ 1970 CE, cyanobacterial ASVs increased again and continuously remained > 50 % with further peaks ~ 1993 CE and ~ 2005 CE.

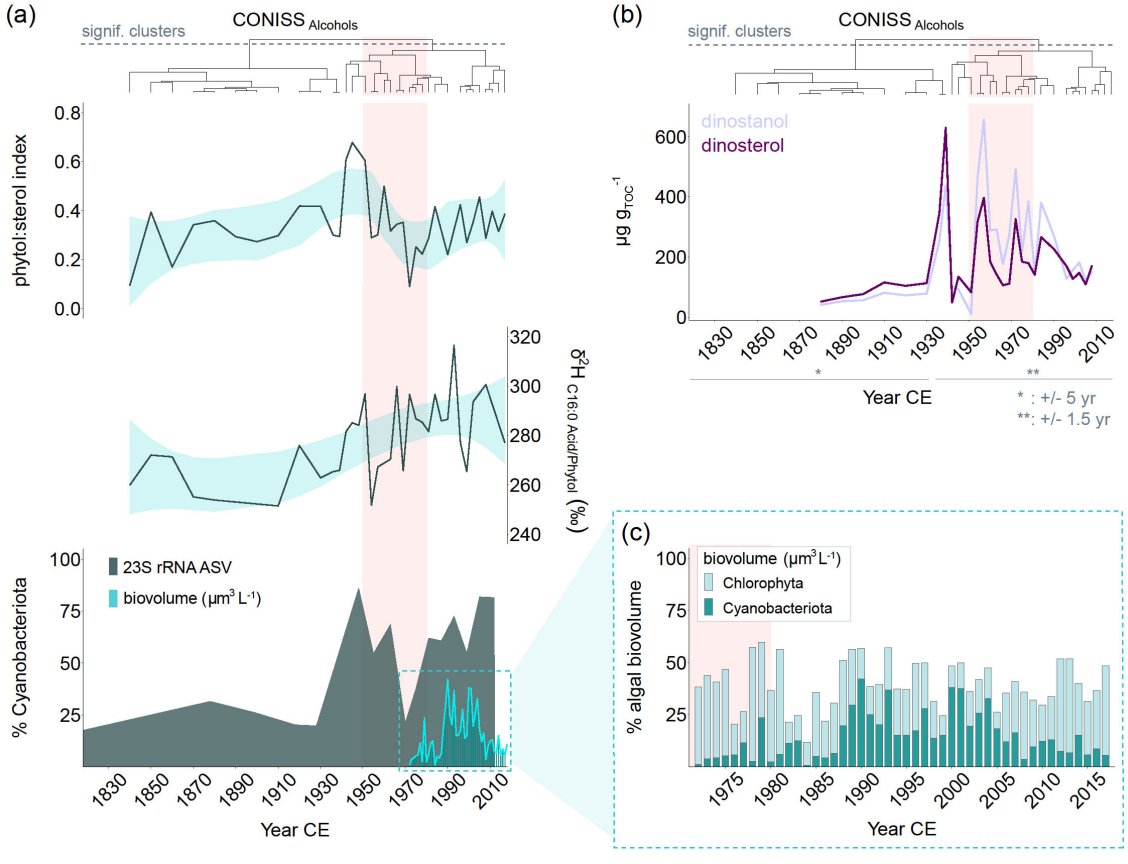

Figure 2: Time series of different proxies for phytoplankton community composition in Greifensee. (a) Phytol:sterol index values (shaded areas represent 95 % confidence intervals of LOESS span = 0.5 fit), $\delta^2H_{C16:0\ Acid/Phytol}$ values (LOESS span = 0.9 fit) and relative abundance of cyanobacterial 23S rRNA amplicon sequence variants (ASVs). Changing lipid sources are indicated by a CONISS cluster dendrogram of relative alcohol distributions. ASVs are plotted with cyanobacterial biovolume in the water column based on mean annual cell counts from Bürgi et al. (2003) and Merz et al. (2023). (b) Dinostanol and dinosterol

https://doi.org/10.5194/egusphere-2026-4300
Preprint. Discussion started: 24 August 2026

concentrations plotted with the CONISS cluster of alcohol distributions. (c) Relative biovolume of Chlorophyta and Cyanobacteriota in the water column based on mean annual cell counts from Bürgi et al. (2003) and Merz et al. (2023). The biovolume of Chlorophyta is included for the interpretation of $\delta^2H_{C16:0\ Acid/Phytol}$ values. Red background shading indicates the period of maximum eutrophication (~ 1950 to 1980 CE).

On the taxonomic class level, 23S rRNA ASVs during the 1800s and the early 1900s derived mainly from Bangiophyceae (Rhodophyta) and Trebouxiophyceae (Chlorophyta) in addition to the stable proportion of ASVs of Cyanophyceae (Fig. 3). Single samples displayed higher abundances of ASVs from Euglenida. The strong increase of Cyanophyceae in ~ 1948 CE co-occurred with a significant shift in ASV clusters. Within eukaryotic algal classes, high abundances of 23S rRNA ASVs from Eustigmatophyceae were found until the 1980s, while the abundance of ASVs from Trebouxiophyceae remained generally high with a particular peak ~ 1970 CE.

https://doi.org/10.5194/egusphere-2026-4300
Preprint. Discussion started: 24 August 2026

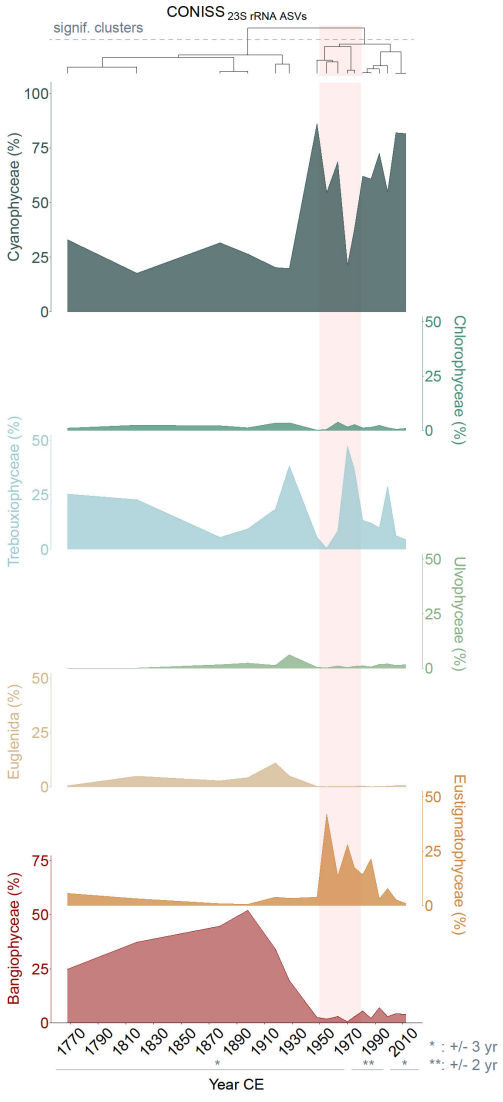

Figure 3: Time series of the relative abundances of different algal classes in Greifensee, based on taxonomic assignments of 23S rRNA amplicon sequence variants (ASVs), plotted with a CONISS cluster dendrogram of ASV distributions. Algal classes comprising less than 20 % in all samples are not shown. Red background shading indicates the period of maximum eutrophication (~ 1950 to 1980 CE).

https://doi.org/10.5194/egusphere-2026-4300
Preprint. Discussion started: 24 August 2026

3.2 Murtensee

In Murtensee, the PSI was stable and relatively low from the mid-1800s until ~ 1940 and strongly increased ~ 1946 CE, co-occurring with significant changes in clusters of sedimentary alcohol distributions (Fig. 4a). The PSI remained high until the early 2000s and slightly decreased afterwards, consistent with changes in alcohol distributions.

$\delta^2H_{C16:0\ Acid/Phytol}$ values ranged from 137 ‰ in ~ 1910 to 285 ‰ in ~ 1984 CE (Fig. 4a). $\delta^2H_{C16:0\ Acid/Phytol}$ values fluctuated between ~ 140 ‰ and 200 ‰ from the late 1800s until ~ 1937 CE and displayed a first peak with 237 ‰ in ~ 1946 CE co-occurring with significant changes in alcohol clusters. Around 1958 CE, $\delta^2H_{C16:0\ Acid/Phytol}$ values strongly increased and remained > 260 ‰ for the rest of the record.

The abundance of 23S rRNA ASVs of Cyanobacteriota was relatively high during the late 1800s with 72 % in 1873 and > 60 % until the 1900s (Fig. 4a). In ~ 1922 CE, the relative abundance of cyanobacterial ASVs dropped to 18 %, but strongly increased again reaching a peak of almost 80 % ~ 1958 CE. ASVs of Cyanobacteriota then decreased again below 40 % but reached another peak in ~ 1995 CE.

https://doi.org/10.5194/egusphere-2026-4300
Preprint. Discussion started: 24 August 2026

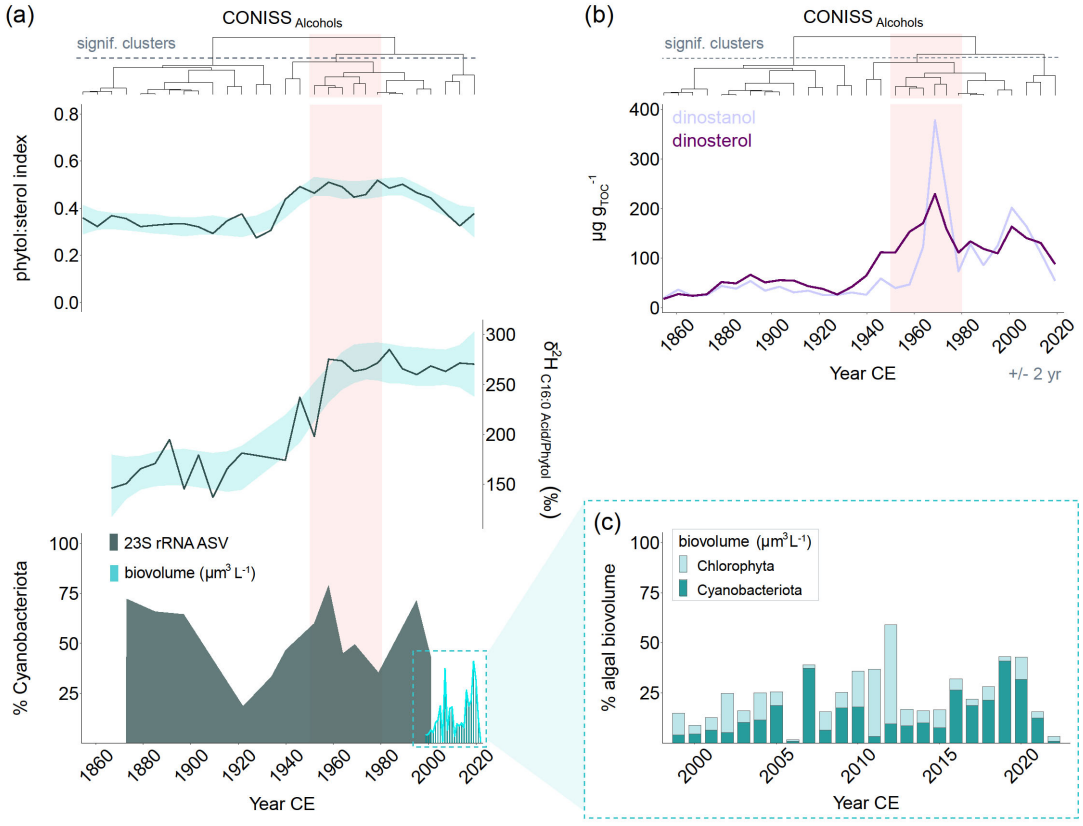

Figure 4: Time series of different proxies for phytoplankton community composition in Murtensee. (a) Phytol:sterol index values (shaded areas represent 95 % confidence intervals of LOESS span = 0.4 fit), $\delta^2H_{C16:0\ Acid/Phytol}$ values (LOESS span = 0.5 fit) and relative abundance of cyanobacterial 23S rRNA amplicon sequence variants (ASVs). Changing lipid sources are indicated by a CONISS cluster dendrogram of relative alcohol distributions. ASVs are plotted with cyanobacterial biovolume in the water column based on mean annual cell counts from Merz et al. (2023). (b) Dinostanol and dinosterol concentrations plotted with the CONISS cluster of alcohol distributions. (c) Relative biovolume of Chlorophyta and Cyanobacteriota in the water column based on mean annual cell counts from Merz et al. (2023). The biovolume of Chlorophyta is included for the interpretation of $\delta^2H_{C16:0\ Acid/Phytol}$ values. Red background shading indicates the period of maximum eutrophication (~ 1950 to 1980 CE).

On the taxonomic class level, smaller proportions of 23S rRNA ASVs during the late 1800s derived from Trebouxiophyceae and minor contributions were from Bangiophyceae in addition to the major abundance of cyanobacterial ASVs (Fig. 5). The proportion of ASVs from Ulvophyceae peaked ~ 1922 CE (33 %). Increasing abundances of cyanobacterial ASVs co-occurred with higher proportions of 23S rRNA ASVs from Eustigmatophyceae. In the 1960s, the abundance of diatom classes increased and ASVs from Fragilariophyceae comprised 49 % in the youngest sample from ~ 2001 CE.

https://doi.org/10.5194/egusphere-2026-4300
Preprint. Discussion started: 24 August 2026

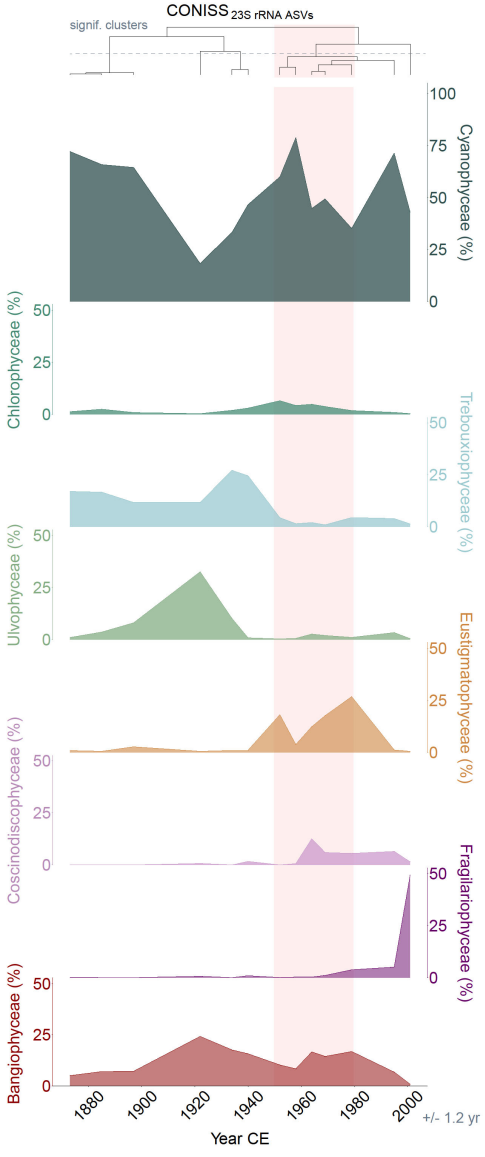

Figure 5: Time series of the relative abundances of different algal classes in Murtensee, based on taxonomic assignments of 23S rRNA amplicon sequence variants (ASVs), plotted with a CONISS cluster dendrogram of ASV distributions. Algal classes comprising less than 20 % in all samples are not shown. Red background shading indicates the period of maximum eutrophication (~ 1950 to 1980 CE).

https://doi.org/10.5194/egusphere-2026-4300
Preprint. Discussion started: 24 August 2026

3.3 Zugersee

For Zugersee, separate sediment cores were analyzed from the northern and the southern basin due to the large differences in their bathymetry, lake depth and water column chemistry, as well as topographical differences within the catchment area (Fig. S2a). In the southern basin, the record of algal proxies begins only ~ 1925 CE due to disruption of the sediment chronology by turbidites (Fig. S2b). These turbidites formed after massive rainfall events, which caused fluvial sedimentation of sandy and siltic material at the lake bottom associated with the steep bathymetry of the shoreline of the southern basin (Fig. S2a) (AquaPlus, 2001).

In the northern basin, the PSI was relatively low and stable in the oldest sample from ~ 1789 CE, during the 1800s until ~ 1940 CE (Fig. 6a). Then, PSI values strongly increased at the same time that alcohol distribution clusters change significantly ~ 1939 CE, and remained high afterwards until the early 2000s. In the southern basin, the PSI increased in the 1950s co-occurring with a significant change in alcohol distributions. PSI values peaked ~ 1977 CE and remained relatively high in the early 2000s as in the northern basin.

The abundance of 23S rRNA ASVs of Cyanobacteriota was low in the oldest samples of the northern basin, with < 1 % in ~ 1789 CE, and < 20 % until ~ 1901 CE (Fig. 6a). In the early 1900s (~ 1900 to 1940 CE), the abundance of cyanobacterial ASVs slightly increased to > 20 %, and then strongly increased after ~ 1950 CE and remained high afterwards. A first peak in 23S rRNA ASVs of Cyanobacteriota was detected ~ 1961 CE (74 %) and a second peak ~ 1998 CE (95 %). In the southern basin, the abundance of cyanobacterial 23S rRNA ASVs was low to moderate in the early 1900s to ~ 1950 CE, ranging from 13 % to 35 % (Fig. 6a). Similar to the northern basin, the abundance of cyanobacterial ASVs strongly increased after ~ 1950 CE and peaked to 76 % in ~ 1956 CE. Afterwards, 23S rRNA ASVs of Cyanobacteriota slightly decreased until ~ 1985 CE, but reached > 90 % in the 2000s.

https://doi.org/10.5194/egusphere-2026-4300
Preprint. Discussion started: 24 August 2026

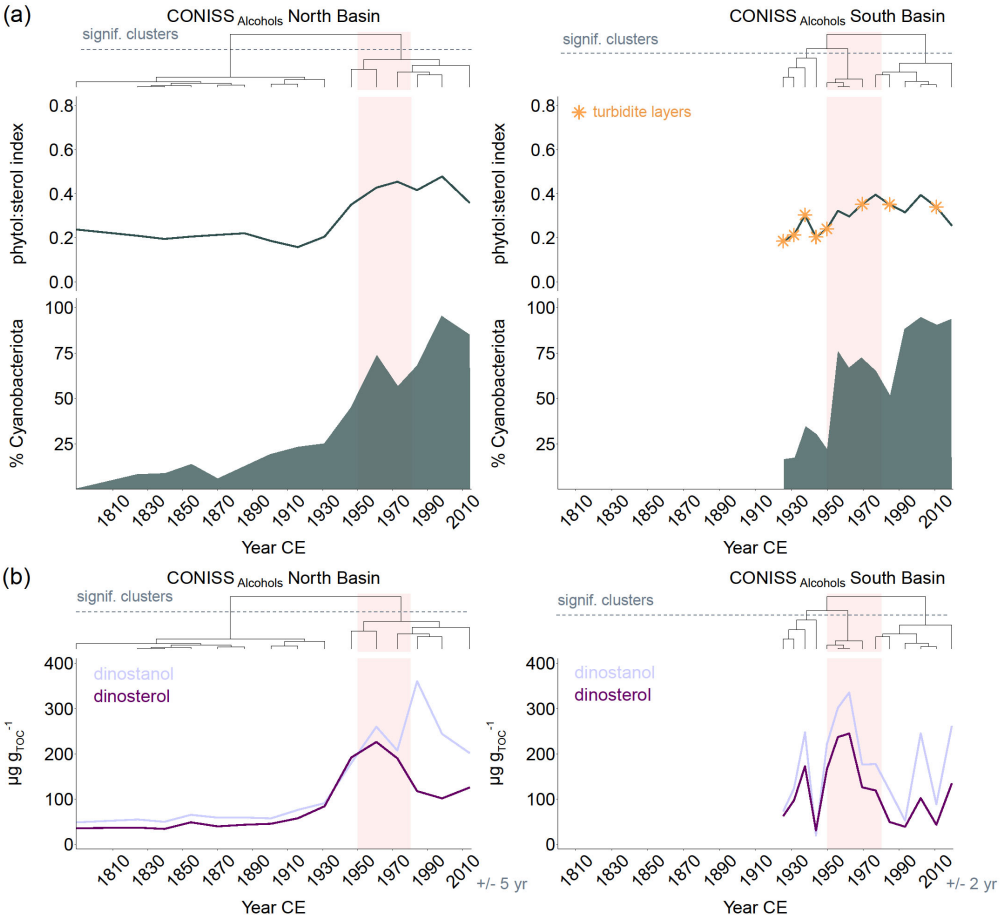

Figure 6: Time series of different proxies for phytoplankton community composition in the northern (left) and southern (right) basin of Zugersee. (a) Phytol:sterol index values and relative abundance of cyanobacterial 23S rRNA amplicon sequence variants (ASVs). Changing lipid sources are indicated by a CONISS cluster dendrogram of relative alcohol distributions. (b) Dinostanol and dinosterol concentrations along the CONISS cluster of alcohol distributions. Red background shading indicates the period of maximum eutrophication (~ 1950 to 1980 CE).

On the taxonomic class level, 23S rRNA ASVs in the oldest samples from the northern basin derived mainly from Bangiophyceae, but green algal taxa, i.e. Trebouxiophyceae and Ulvophyceae increased in the early to late 1800s varying between 15 % and > 30 % (Fig. 7a). In the early 1900s (~ 1900 to 1940 CE), the relative abundance of ASVs from Bangiophyceae increased again, comprising major proportions of eukaryotic algal ASVs. In the mid-1900s, the increase of cyanobacterial ASVs co-occurred with a significant change in ASV clusters and changes in the distributions of eukaryotic

https://doi.org/10.5194/egusphere-2026-4300
Preprint. Discussion started: 24 August 2026

algal ASVs. The proportion of ASVs from Bangiophyceae decreased and eukaryotic algal ASVs derived mainly from Trebouxiophyceae as well as Chlorophyceae and Eustigmatophyceae. In the southern basin, high proportions of 23S rRNA ASVs derived from Trebouxiophyceae ~ 1925 to 1950 CE and single samples displayed relatively high abundances of ASVs from Eustigmatophyceae and Ulvophyceae (Fig. 7b). Similar to the northern basin, the strong increase of cyanobacterial 23S rRNA ASVs ~ 1956 CE co-occurred with a significant change in ASV clusters. Simultaneously, the relative proportions of ASVs from Chlorophyceae peaked during the 1960s to almost 20 %. In samples from the late 1900s with highest abundance of cyanobacterial ASVs, the small proportion of eukaryotic algal ASVs derived mainly from Eustigmatophyceae and Trebouxiophyceae, comparable to samples from the northern basin.

https://doi.org/10.5194/egusphere-2026-4300
Preprint. Discussion started: 24 August 2026

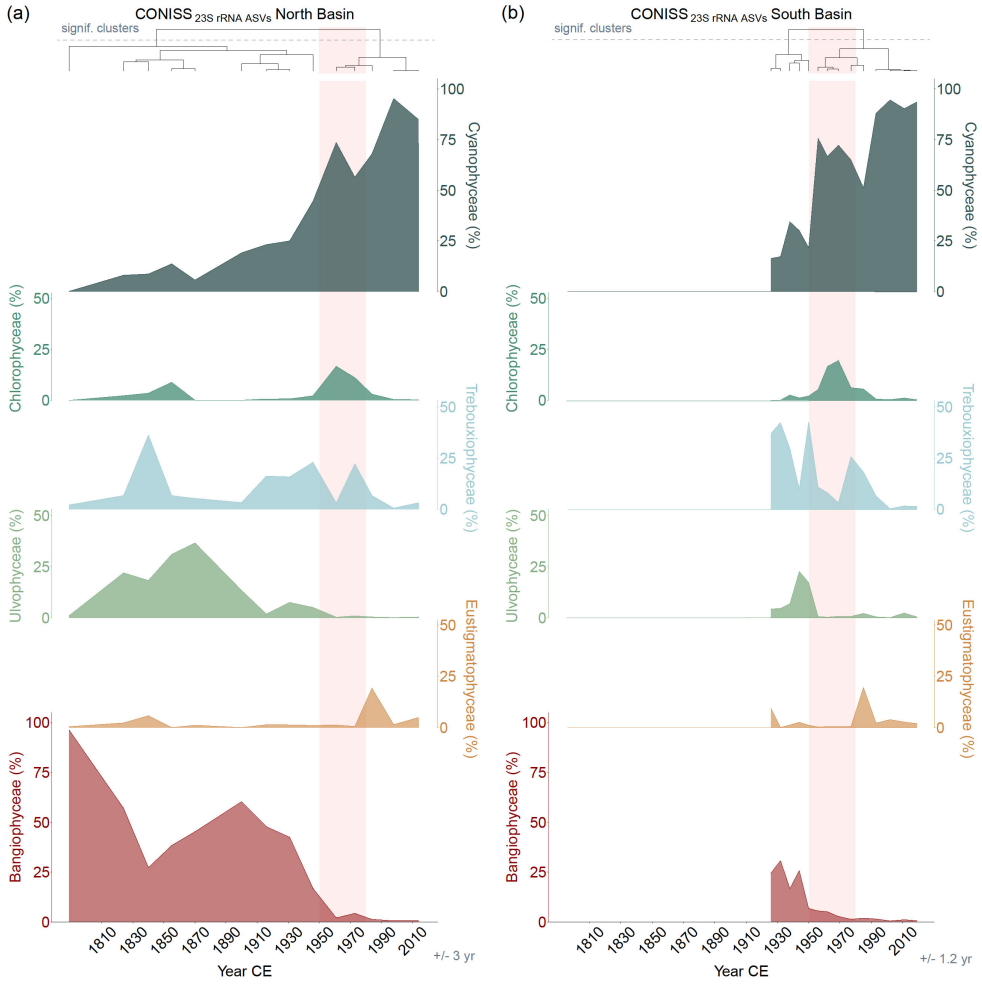

Figure 7: Time series of the relative abundances of different algal classes in the northern (a) and southern (b) basin of Zugersee, based on taxonomic assignments of 23S rRNA amplicon sequence variants (ASVs). ASVs are plotted along a CONISS cluster dendrogram of ASV distributions. Algal classes comprising less than 20 % in all samples are not shown. Red background shading indicates the period of maximum eutrophication (~ 1950 to 1980 CE).

To compare the (dis-)similarities between phytoplankton community compositions in the northern and the southern basin of Zugersee, we performed NMDS analysis of lipid distributions as well as algal 23S rRNA gene ASVs distributions on the taxonomic class level (Fig. 8).

https://doi.org/10.5194/egusphere-2026-4300
Preprint. Discussion started: 24 August 2026

The NMDS of alcohol distributions showed a temporal separation between samples (Fig. 8a). Samples from the 1800s (northern basin) and the early 1900s (~ 1900 to 1940 CE) were separated from samples from the mid- to late 1900s and 2000s along NMDS axis 1, except for two samples derived from turbidites. Along NMDS axis 2, samples from the 1950s and 1960s clustered mostly separately from samples derived from the late 1900s and 2000s. Samples derived from turbidites in the southern basin, clustered together, but mostly showed the same temporal distribution as other samples.

NMDS of 23S rRNA gene ASVs also displayed a temporal clustering with samples from the 1800s (northern basin), early 1900s (~ 1900 to 1940 CE) and late 1940s being mostly separated from samples originating from the mid-1900s to 2000s along NMDS axis 1 (Fig. 8b). Samples from the 1950s to 1980s clustered separately from samples derived from the 1990s and 2000s along NMDS axis 2.

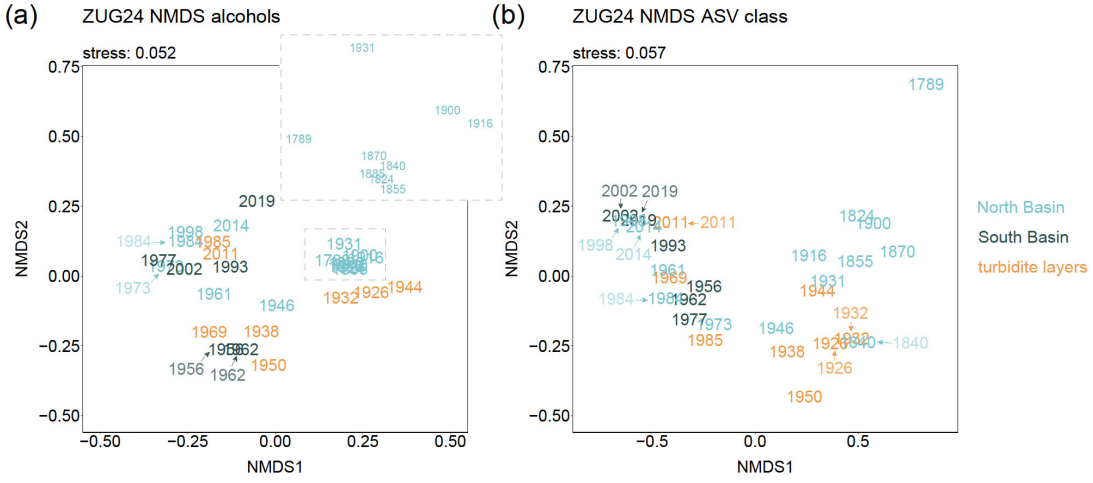

Figure 8: Non-metric-multidimensional scaling (NMDS) of relative alcohol concentrations (a) and algal 23S rRNA amplicon sequence variants (ASVs) distributions (b) in Zugersee in relation to mean sample ages (CE). Sample names refer to the mean age of the respective sample. ASVs were square root transformed prior to analysis. Only the first and second dimensions are shown. For better visualization, arrows mark the exact positions of some samples, and their respective ages are plotted with a slight offset. In (a), the exact positions of single samples (dashed box) are additionally plotted with higher resolution.

4 Discussion

We analyzed alcohol distributions, PSI and $\delta^2H_{C16:0\ Acid/Phytol}$ values along with algal 23S rRNA ASVs in sediment cores of Swiss Plateau lakes to reconstruct changes of phytoplankton communities in response to strong eutrophication during the 20th century. In the following discussion, we compare the various lipid proxies with algal ASVs and cross-validate these proxies with observational limnological studies, available cell count data (Greifensee and Murtensee), algal pigment distributions (Murtensee), and changes in diatom communities (Zugersee).

https://doi.org/10.5194/egusphere-2026-4300
Preprint. Discussion started: 24 August 2026

4.1 Comparison between lipid proxies and algal 23S rRNA ASVs

In all studied lakes, sedimentary lipid proxies and algal 23S rRNA ASVs indicated significant changes in the algal community associated with the strong eutrophication period of the 20th century (Fig. 2 to 7). The overall timing of significant changes in alcohol clusters was consistent with changes in ASV clusters. Regarding changing proportions of cyanobacteria and eukaryotic algae, PSI and $\delta^2H_{C16:0\ Acid/Phytol}$ values recorded generally the same trends as cyanobacterial and eukaryotic algal plastid 23S rRNA ASVs. In the 1800s and early 1900s, low relative abundance of cyanobacterial ASVs, as well as low PSI and $\delta^2H_{C16:0\ Acid/Phytol}$ values suggest minor proportions of cyanobacteria. Additionally, the high relative abundances of ASVs from macroalgae (i.e., Bangiophyceae and Ulvophyceae) imply low phytoplankton productivity in the water column consistent with oligotrophic lake conditions. However, the high proportion of Bangiophyceae and Ulvophyceae ASVs in single samples was represented by only one single amplicon variant which may reflect biases from PCR overamplification (Best et al., 2015). During the early eutrophication phase in the 1940s, PSI and $\delta^2H_{C16:0\ Acid/Phytol}$ values strongly increased, consistent with increasing relative abundance of cyanobacterial ASVs, indicating a shift of algal community composition towards higher proportions of cyanobacteria.

Nevertheless, some discrepancies were found between cyanobacterial lipid proxies and ASVs in Greifensee and Murtensee. In Greifensee, the PSI, $\delta^2H_{C16:0\ Acid/Phytol}$ values and cyanobacterial ASVs displayed clear peaks during the 1940s. However, PSI values decreased afterwards and remained comparably low until the 2000s, while $\delta^2H_{C16:0\ Acid/Phytol}$ values and cyanobacterial ASVs increased again and remained high during the 1980s and 1990s. High $\delta^2H_{C16:0\ Acid/Phytol}$ values are indicative for cyanobacteria when they are associated with a strong ^{2}H-depletion of phytol (Ladd et al., 2025). However, in Greifensee, the increase in $\delta^2H_{C16:0\ Acid/Phytol}$ values during the 1980s was mainly due to the ^{2}H-enrichment of C16:0 fatty acid (Fig. S5a). The ^{2}H-enrichment of C16:0 fatty acid co-occurring with peaks of the bacterial hopanoid diplopterol (Fig. S5b) (Ourisson et al., 1987) could reflect high biomass from heterotrophic bacteria, which tend to have higher $\delta^2H_{C16:0\ Acid}$ values than photoautotrophs (Zhang et al., 2009, Heinzelmann et al., 2015; Wijker et al., 2019). In addition to heterotrophic bacterial biomass, ^{2}H-enrichment of C16:0 fatty acid might be related to high biovolume of green algae during the late 1960s and early 1970s (Fig. 2c) (Sect. 4.2) (Ladd et al., 2025).

In Murtensee, PSI and $\delta^2H_{C16:0\ Acid/Phytol}$ values were low during the 1800s until the 1940s, while ASVs of Cyanobacteriota comprised the majority of algal ASVs (Fig. 4a). On the genus level, cyanobacterial ASVs in Murtensee during the late 1800s were assigned mainly to *Synechococcus* (Fig. S6b). Despite their small cell size, coccoid cyanobacterial genera like *Synechococcus* can exhibit high DNA amounts due to polyploidy of their chromosomes (Watanabe, 2020). In case of generally low algal productivity associated with low abundances of eukaryotic algal ASVs, multiple copies of cyanobacterial chromosomes per single cell can overestimate the actual abundance of cyanobacteria within the community, leading to discrepancies between lipid proxies and 23S rRNA ASVs. After the 1940s, PSI and $\delta^2H_{C16:0\ Acid/Phytol}$ values remained high. Cyanobacterial ASVs peaked ~ 1958 CE, but decreased during the 1960s and 1970s (Fig. 4a). In line with the assumption of

https://doi.org/10.5194/egusphere-2026-4300
Preprint. Discussion started: 24 August 2026

high DNA amounts in small coccoid cyanobacteria, decreasing cyanobacterial ASVs were associated with lower abundances of *Synechococcus*.

Besides the good temporal agreement of significant changes in sedimentary alcohol and ASV clusters, the representations of specific algal groups by the two different proxies differ from each other. Dinosterol and dinostanol, commonly used as a proxy for dinoflagellates (e.g., Meyers and Ishiwatari, 1993; Volkman, 2003), were found in sediment samples from all lakes, and generally increased with lake eutrophication (Fig. 2b; Fig. 4b; Fig. 6b). In contrast, algal 23S rRNA ASVs from Dinophyceae were always low. Contrasting results between dinosterol and *sed*DNA have been reported by other studies, in which these discrepancies have been related to the variability of dinosterol production among different dinoflagellate species (Boere et al, 2011; Romahn et al., 2025). Moreover, dinosterol could potentially be synthesized by other algal groups (e.g., diatoms) (Volkman et al., 1993). However, the past abundance of dinoflagellates in Murtensee and Zugersee is reflected by algal pigments (Makri et al., 2019) and reported in historical observations (Brutschy, 1912) contradicting other algal sources of dinosterol as well as the low abundance of Dinophyceae reflected by ASVs. In the early 1900s, the dinoflagellate *Ceratium hirundinella* was even described as a "characteristic plankton form" in Zugersee which "never [..] disappears" (Brutschy, 1912). The underestimation of dinoflagellate abundance by plastid 23S rRNA ASVs may be related to the unique fragmented organization of their plastid genome and associated difficulties in properly amplifying dinoflagellate plastid rRNA genes (Sherwood and Presting, 2007; Xu et al., 2023; Tang et al., 2024).

Moreover, low specificity of taxonomic assignments by NCBI, as implied by the scattered distribution of algal phyla in the phylogenetic tree (Fig. S7), could be an additional factor leading to the missing representation of dinoflagellates. Dinoflagellate plastids evolutionarily originate from secondary endosymbiosis of red algae (Zhang et al., 1999; Zhang et al., 2000; Tang et al., 2024). Although *Bangia atropurpurea*, the only freshwater species of Bangiophyceae, has been reported in Swiss lakes as part of the benthic community in the littoral zone (Thomas 1960), red algae comprise mainly marine species (Sheath and Wehr, 2015). Therefore, the high abundance of Bangiophyceae 23S rRNA ASVs before eutrophication could reflect inaccurate taxonomic assignments of peridinin-containing dinoflagellates.

4.2 Cross-validation of sedimentary algal proxies with documented changes in phytoplankton communities

Phytoplankton community changes in Greifensee, Murtensee and Zugersee have been documented by other studies based on diatom frustules, sedimentary pigments, and single qualitative observations in the water column (Brutschy, 1912; Soracreppa, 1978; AquaPlus, 2001; Bürgi et al., 2003; Makri et al., 2019). For Greifensee and Murtensee, quantitative algal cell counts are available for specific time periods (Bürgi et al., 2003; Merz et al., 2023). Based on these cell counts, the biovolume of individual phytoplankton groups was calculated (Fig. S8; Fig. S10) which is suitable for the cross-validation of sedimentary proxies. However, samples for algal cell counts do not comprise the whole water column and reflect the algal community at specific sampling dates and locations. In contrast, sediment archives incorporate changes over multiple years as a more integrative signal from the whole water column (e.g., Thorpe et al., 2024; Romahn et al., 2025). Moreover,

https://doi.org/10.5194/egusphere-2026-4300
Preprint. Discussion started: 24 August 2026

taphonomic processes as well as degradation of algal material impact the transition of the water column signal to the sediment (e.g., Thorpe et al., 2024). Therefore, we do not focus on species biovolume on the yearly scale, but rather overall changes in algal community compositions on higher taxonomic levels.

During the mid-1960s, the algal community in Greifensee was described as a fluctuating co-existence of Cyanobacteriota, Chlorophyta and Chromophyta (Soracreppa, 1978), consistent with decreasing PSI values, as well as low cyanobacterial ASVs in 1969 CE (Fig. 2a). Phytoplankton biovolume in the water column of Greifensee displayed relatively high proportions of green algal taxa in the early 1970s, specifically Chlorophyceae, and further showed an increase of cyanobacterial biovolume during the late 1980s (Fig. 2c; Fig. S8) (Bürgi et al., 2003; Merz et al., 2023). The relatively high proportions of green algal biovolume are also consistent with high $\delta^2H_{C16:0\ Acid/Phytol}$ values compared to rather low PSI values in sediment samples. Likewise, high proportions of sedimentary 23S rRNA ASVs derived from green algae (Fig. 3), but in contrast to algal cell counts, green algal ASVs in the sediment were mostly assigned to Trebouxiophyceae with negligible proportions of Chlorophyceae. These differences in the representation of Chlorophytes by *sed*DNA and microscopic cell counts have also been shown by Thorpe et al. (2024), with microscopy generally capturing more taxa. Regarding eukaryotic algal groups in general, cell counts documented the persistent abundance of Cryptophyceae which were mostly not reflected by sedimentary algal ASVs. The poor preservation of Cryptophyceae DNA in sediment records may be associated with preferential DNA degradation due because they do not have a cell wall as well as selective zooplankton grazing (Capo et al., 2015; Thorpe et al., 2024).

The increasing proportions of cyanobacterial biovolume in the water column during the late 1980s were also indicated by moderately increasing PSI values, however, cyanobacterial 23S rRNA ASVs strongly increased in sediment samples (Fig. 2a). Cell counts mainly documented the abundance of Chroococcoides and Synechococcales, and ASVs were mostly assigned to Synechococcales (Fig. S6a). The low biovolume of these small coccoid cells relative to high DNA amounts might result in relatively low PSI values in contrast to high abundance of cyanobacterial ASVs, similar to what was observed in the late 19th century in Murtensee (Sect. 4.1) (Watanabe, 2020).

In Murtensee, the analyses of sedimentary pigment distributions from Makri et al. (2019) indicated increasing proportions of cyanobacteria in response to eutrophication ~ 1937 CE, with oscillaxanthin specifically reflected the abundance of *Planktothrix rubescens* and other filamentous cyanobacteria (Fig. S9). This is consistent with significant changes in alcohol clusters as well as the strong increase in PSI and $\delta^2H_{C16:0\ Acid/Phytol}$ values ~ 1940s. Pigment zones further indicated a shift from filamentous to colonial taxa during the 1970s (Makri et al., 2019). However, peaks in cyanobacterial 23S rRNA ASVs ~ 1958 CE were assigned to *Synechoccocus* while ASVs from the order Oscillatoriales were almost absent. Although 23S rRNA genes of Oscillatoriales have been successfully amplified in the water column and algal mats of lakes (Steven et al., 2012), their absence in sediment samples of Murtensee might indicate preferential degradation.

Pigment zones indicated less cyanobacteria from 1983 CE to 2014 CE associated with strong zooplankton grazing reflected by astaxanthin (Makri et al., 2019). In contrast, the sediment samples in our study displayed peaks in cyanobacterial ASVs ~ 1995 CE and high PSI and $\delta^2H_{C16:0\ Acid/Phytol}$ values reflect high cyanobacterial abundance during the early 2000s (Fig. 4a).

https://doi.org/10.5194/egusphere-2026-4300
Preprint. Discussion started: 24 August 2026

Generally, phytol and phytosterols can be preserved in zooplankton fecal pellets, the latter as steryl chlorin esters (Prahl et al., 1984; Pearce et al., 1998), while xanthophylls can be prone to degradation in some zooplankton types (e.g., Pandolfini et al., 2000). Therefore, PSI and $\delta^2H_{C16:0\ Acid/Phytol}$ values might be less impacted by grazing. Still, biovolume calculations based on algal cell counts from Merz et al. (2023) indicated low to moderate proportions of cyanobacterial biovolume during the early 2000s (Fig. 4a, c; Fig. S10). Additionally, phytoplankton biovolume comprised relatively high proportions of Bacillariophyceae and Chrysophyceae (Fig. S10). Uncertainties regarding the relative abundance of phytol and phytosterols in these eukaryotic algae, as well as a lack of $\delta^2H_{C16:0\ Acid/Phytol}$ values for Chrysophyceae (Klatt et al., 2025; Ladd et al., 2025), might explain the discrepancies between sedimentary lipid proxies and phytoplankton biovolume. Alternatively, cell counts from Murtensee, which comprised 0 to 10 m and 0 to 12 m water depth (Merz et al., 2023), might not be fully representative for the whole water column and cyanobacteria potentially thriving at deeper water depths might have been missed (e.g., Takasu et al., 2015; Klatt et al., 2025).

In Zugersee, sedimentary alcohol and algal ASV clusters reflected significant changes in algal community composition ~ 1940 CE and PSI values further indicated the increasing abundance of cyanobacteria in response to eutrophication (Fig. 6a). Likewise, limnological studies in the early 1900s documented generally low abundance of Cyanophyceae and high quantities of dinoflagellates, despite single winter and spring blooms of *Planktothrix rubescens* (Brutschy, 1912). In contrast, later phytoplankton studies from the mid-1960s described Cyanobacteriota as the main algal group in the North basin of Zugersee (Soracreppa, 1978).

Regarding the two different basins of Zugersee, NMDS of alcohol and 23S rRNA ASV distributions displayed no site-specific differences, but rather a temporal clustering that separated samples from the 1800s and early 1900s (~ 1900s to 1940 CE) from samples derived from the mid- to late 1900s and 2000s (Fig. 8). This suggests that phytoplankton community composition and changes in response to eutrophication were similar among the North and South basin, despite the large differences in water chemistry and bathymetry of the two basins (Fig. S2) (Brutschy, 1912; Dittrich 2009; Maerki et al., 2009). This is in accordance with early phytoplankton observations from Brutschy (1912) which concluded that Zugersee is a 'biological uniform basin' regardless of some differences in plankton quantities and single bloom events.

Although the sediment record from the southern basin in our study did not span the early 1900s, the similarity with the northern basin is additionally reflected by shifts in diatom assemblages (Fig. S11) (AquaPlus, 2001). The published sediment record of diatom frustules from the southern basin displayed a strong increase of eutrophic species, i.e., *Tabellaria flocculosa, Fragilaria crotonensis* und *Stephanodiscus parvus* ~ 1950 CE (AquaPlus, 2001). Considering uncertainties in age determination of sediment cores, this shift in the diatom community of the southern basin likely co-occurred with the significant changes in alcohol clusters as well as increasing abundance of cyanobacteria in the northern basin (Fig. 6a).

4.3 Recommendations for the application and interpretation of algal proxies in sediment records

In all studied lakes, sediment records of algal lipid proxies and algal 23S rRNA ASVs reflected significant changes in phytoplankton community compositions in response to anthropogenic eutrophication, and indicated that this eutrophication

https://doi.org/10.5194/egusphere-2026-4300
Preprint. Discussion started: 24 August 2026

was associated with increases in the relative proportions of cyanobacteria (Fig. 2 to 7). In general, PSI and $\delta^2H_{C16:0\ Acid/Phytol}$ values reflected the same trends as algal 23S rRNA ASVs regarding the relative proportions of cyanobacteria and eukaryotic algae on the phylum level. Nevertheless, each sedimentary proxy has its own biases and limitations which need to be considered for the robust reconstruction of phytoplankton community compositions in the past.

Specifically, the abundance of small coccoid cyanobacterial cells, i.e. *Synechococcus* and *Chroococcus*, might be underestimated by the PSI due to their comparably low biovolume. Generally, PSI values could be also biased by allochthonous phytol and phytosterol sources, therefore, the PSI should be always interpreted in combination with overall sedimentary alcohol distributions.

Likewise, other lipid sources besides phytoplankton also impact the interpretation of $\delta^2H_{C16:0\ Acid/Phytol}$ values and fluctuations of $\delta^2H_{C16:0\ Acid/Phytol}$ values should be additionally assessed by the individual δ^2H_{Lipid} values. For instance, the ^2H-enrichment of δ^2H values of C16:0 fatty acid can be related to higher relative proportions of green algae (Ladd et al., 2025) but might also reflect contributions from heterotrophic bacteria (Zhang et al., 2009, Heinzelmann et al., 2015; Wijker et al., 2019). Hence, the analysis of bacterial biomarkers, like diplopterol as well as iso- and anteiso-branched short-chain fatty acids (e.g., Perry et al., 1979; Ourisson et al., 1987) alongside $\delta^2H_{C16:0\ Acid}$ values is preferable. Additionally, on longer time scales or through periods of major hydrologic or climatic transitions, changes in δ^2H values of source water need to be considered when interpreting individual δ^2H_{Lipid} values.

The lipid-based proxies for algal community composition were generally consistent with algal 23S rRNA ASVs in the sediment, however, cyanobacterial ASVs have been shown to overestimate the abundance of small coccoid cyanobacterial cells, likely related to polyploidy of their chromosomes (Watanabe, 2020). Consequently, the relative abundance of cyanobacterial 23S rRNA ASVs should be additionally assessed on the genus level. In contrast, the abundance of dinoflagellates was likely underestimated by 23S rRNA ASVs and alternative primers or other dinoflagellate proxies are recommended. Generally, our study confirmed previous findings regarding the limited representation of Chlorophyceae and Cryptophyceae by *sed*DNA (Capo et al., 2015; Thorpe et al., 2024). The phylogenetic clustering of 23S rRNA ASVs further revealed relatively non-specific taxonomic assignments by the NCBI database (Fig. S7) and alternative plastid-specific databases might be more favorable.

Overall, each proxy is associated with its own limitations, and the sole use of a single proxy does not provide a robust tool to properly reconstruct phytoplankton community composition. Although the analysis of algal *sed*DNA allows taxa to be more highly resolved than they can be with lipid proxies, our study demonstrates potential biases related to preferential degradation, primer choice and the specificity of the reference database. Therefore, we emphasize a multi-proxy approach incorporating multiple lines of evidence for the reconstruction of changes in phytoplankton community compositions in the past.

https://doi.org/10.5194/egusphere-2026-4300
Preprint. Discussion started: 24 August 2026

5 Conclusions

We collected short sediment cores from lakes on the Swiss Plateau (Greifensee, Murtensee, Zugersee) that had experienced severe human eutrophication during the 20th century, causing changes in their phytoplankton community composition. We analyzed sedimentary alcohol distributions, PSI and $\delta^2H_{C16:0\ Acid/Phytol}$ values in combination with cyanobacterial and eukaryotic algal 23S rRNA ASVs to reconstruct relative abundance of eukaryotic algae and cyanobacteria. In general, PSI and $\delta^2H_{C16:0\ Acid/Phytol}$ values were consistent with the relative abundance of cyanobacterial ASVs, indicating increasing proportions of cyanobacteria in response to eutrophication. However, the comparison between lipid proxies and algal ASVs revealed that the abundance of small coccoid cyanobacterial genera might be overestimated by 23S rRNA ASVs relative to their biovolume. Moreover, $\delta^2H_{C16:0\ Acid/Phytol}$ values were potentially impacted by non-algal lipid sources, specifically C16:0 fatty acids of heterotrophic origin. On the other hand, the cross-validation with documented changes in phytoplankton communities indicated that individual eukaryotic algal groups, specifically dinoflagellates, Chlorophyceae and Cryptophyceae are poorly reflected by sedimentary 23S rRNA ASVs.

The overall good agreement between PSI and $\delta^2H_{C16:0\ Acid/Phytol}$ values with algal 23S rRNA ASVs and documented changes of algal communities validates the use of these new lipid-based proxies for reconstructing the relative abundance of cyanobacteria and eukaryotic algae over longer time scales (decades, centuries and millennia). Nevertheless, autochthonous lipid sources other than phytoplankton, as well as allochthonous terrestrial lipid sources, can impact PSI and $\delta^2H_{C16:0\ Acid/Phytol}$ values in sediment records and the combination of multiple algal proxies is always preferable.

Code and data availability

All data of this study are available through the Dryad Digital Repository (https://doi.org/10.5061/dryad.ht76hdrz6) with the exception of raw sequencing reads obtained from *sed*DNA samples, which will be published at the European Nucleotide Archive repository (project number: PRJEB114126). All R scripts and related data files are uploaded in GitHub (https://github.com/antoniaKlatt/Klatt_etal_2026_SwissPlateau_Lakes). Phytoplankton cell counts from Murtensee (Merz et al., 2023) were obtained from the Eawag Research Data Institutional Collection (https://doi.org/10.25678/0007VX). The compiled phytoplankton cell count data from Greifensee (Bürgi et al., 2003; Merz et al., 2023) were obtained upon request from the Department Aquatic Ecology at Eawag. Sedimentary diatom assemblages and the respective phosphorus reconstructions from Greifensee and Zugersee were obtained upon request from the corresponding author (AquaPlus, 2001; AquaPlus, 2004). Pigment data from Murtensee were obtained upon request from the corresponding author (Makri et al., 2019).

https://doi.org/10.5194/egusphere-2026-4300
Preprint. Discussion started: 24 August 2026

Author contributions

Conceptualization: AK, SNL, ND; Formal analysis: AK, JW, TW; Funding acquisition: SNL, ND; Investigation: AK, DBN, JW; Methodology: AK, SNL, DBN, JW; Project administration: SNL, ND; Supervision: SNL; Visualization: AK; Writing – original draft: AK; Writing - review & editing: All.

Competing interests

The authors declare that they have no conflict of interest.

Acknowledgements

Adrian Gilli, Anita Schlatter, Pascal Rünzi, Ricardo N. Santos, Michelle Patrice Engelhardt, Antoine De Clippele, Ronald Lloren, Nannan Li, Markus Möst, Tobias Schneider, Patrick Kathriner and Pasqualina Vonlanthen DiNenna assisted with fieldwork. David Janssen assisted with fieldwork coordination. Axel Birkholz, Sandra Schmid and Shannon Dyer assisted with extractions, purifications and analyses of lipid samples. Nico Scheurer, Charlotte Duda and Abigail Gex-Collet assisted with subsampling, sample preparation for sediment dating and purifications of lipid samples. Fabian Rey assisted with core splitting and coordination of *sed*DNA subsampling. Pascal Rünzi performed ^{210}Pb, ^{226}Ra ^{137}Cs measurements. Jakob Zopfi and Nathalie Amacker assisted with *sed*DNA extractions. Christine Alewell, Moritz Lehmann and Ansgar Kahmen provided laboratory space and access to instrumentation.

The Genomics Facility Basel, operated by the University of Basel and the Department of Biosystems Science and Engineering (D-BSSE), ETH Zurich, performed library preparation and amplicon sequencing of *sed*DNA samples and amplicon sequencing data were processed at the sciCORE (http://scicore.unibas.ch/) scientific computing core facility at University of Basel.

The Swiss Federal Office for the Environment (FOEN) provided phosphorus measurement data of the different lakes from AWEL Zurich, canton Fribourg and canton Zug. Joachim Hürlimann (AquaPlus) provided sedimentary diatom count data and diatom-based phosphorus reconstructions from Greifensee and Zugersee. Stamatina Makri provided pigment data from Murtensee. Marta Reyes provided compiled phytoplankton cell count data from Bürgi et al. (2003) and Merz et al. (2023) and species-specific phytoplankton biovolume measurements from H. Bürgi.

Financial support

This research was funded by a Swiss National Science Foundation (SNSF) Eccellenza Fellowship to SNL (PCEFP2 194211), an ETH Zurich Career Seed Award to SNL and Eawag internal funds.

https://doi.org/10.5194/egusphere-2026-4300
Preprint. Discussion started: 24 August 2026

References

AquaPlus: Entwicklung des Gesamtphosphors im Zugersee anhand der im Sediment eingelagerten Kieselalgen, Bericht zuhanden des Amtes für Umweltschutz des Kantons Zug, 2001.

AquaPlus: Entwicklung des Gesamtphosphors im Greifensee anhand der im Sediment eingelagerten Kieselalgen, Bericht zuhanden des Amtes für Abfall, Wasser, Energie und Luft des Kantons Zürich, 2004.

Aquino-López, M. A., Blaauw, M., Christen, J. A., and Sanderson, N. K.: Bayesian Analysis of 210 Pb Dating, J. Agric. Biol. Environ. Stat., 23, 317–333, https://doi.org/10.1007/s13253-018-0328-7, 2018.

Arhonditsis, G. B., Stow, C. A., Steinberg, L. J., Kenney, M. A., Lathrop, R. C., McBride, S. J., and Reckhow, K. H.: Exploring ecological patterns with structural equation modeling and Bayesian analysis, Ecol. Modell., 192, 385–409, https://doi.org/10.1016/j.ecolmodel.2005.07.028, 2006.

Armbrecht, L., Weber, M. E., Raymo, M. E., Peck, V. L., Williams, T., Warnock, J., Kato, Y., Hernández-Almeida, I., Hoem, F., Reilly, B., Hemming, S., Bailey, I., Martos, Y. M., Gutjahr, M., Percuoco, V., Allen, C., Brachfeld, S., Cardillo, F. G., Du, Z., Fauth, G., Fogwill, C., Garcia, M., Glüder, A., Guitard, M., Hwang, J. H., Iizuka, M., Kenlee, B., O'Connell, S., Pérez, L. F., Ronge, T. A., Seki, O., Tauxe, L., Tripathi, S., and Zheng, X.: Ancient marine sediment DNA reveals diatom transition in Antarctica, Nat. Commun., 13, https://doi.org/10.1038/s41467-022-33494-4, 2022.

Atwood, A. R., Volkman, J. K., and Sachs, J. P.: Characterization of unusual sterols and long chain diols, triols, keto-ols and n-alkenols in El Junco Lake, Galápagos, Org. Geochem., 66, 80–89, https://doi.org/10.1016/j.orggeochem.2013.11.004, 2014.

Baan, J., Holloway-Phillips, M., Nelson, D. B., and Kahmen, A.: The metabolic sensitivity of hydrogen isotope fractionation differs between plant compounds, Phytochemistry, 207, https://doi.org/10.1016/j.phytochem.2022.113563, 2023.

Best, K., Oakes, T., Heather, J. M., Shawe-Taylor, J., and Chain, B.: Computational analysis of stochastic heterogeneity in PCR amplification efficiency revealed by single molecule barcoding, Sci. Rep., 5, https://doi.org/10.1038/srep14629, 2015.

Boere, A. C., Sinninghe Damsté, J. S., Rijpstra, W. I. C., Volkman, J. K., and Coolen, M. J. L.: Source-specific variability in post-depositional DNA preservation with potential implications for DNA based paleoecological records, Org. Geochem., 42, 1216–1225, https://doi.org/10.1016/j.orggeochem.2011.08.005, 2011.

Brocks, J. J., Jarrett, A. J. M., Sirantoine, E., Hallmann, C., Hoshino, Y., and Liyanage, T.: The rise of algae in Cryogenian oceans and the emergence of animals, Nature, 548, 578–581, https://doi.org/10.1038/nature23457, 2017.

Brutschy, A.: Monographische Studien am Zugersee, Archiv für Hydrobiologie und Planktonkunde, 8, 43-107, https://doi.org/10.3929/ethz-a-000092314, 1912.

Bürgi, H. R., Bührer, H., and Keller, B.: Long-term changes in functional properties and biodiversity of plankton in Lake Greifensee (Switzerland) in response to phosphorus reduction, Aquat. Ecosyst. Health and Manag., 6,147-158, 2003.

Callahan, B. J., McMurdie, P. J., Rosen, M. J., Han, A. W., Johnson, A. J. A., and Holmes, S. P.: DADA2: High-resolution sample inference from Illumina amplicon data, Nat. Methods, 13, 581–583, https://doi.org/10.1038/nmeth.3869, 2016.

https://doi.org/10.5194/egusphere-2026-4300
Preprint. Discussion started: 24 August 2026

Capo, E., Debroas, D., Arnaud, F., and Domaizon, I.: Is Planktonic Diversity Well Recorded in Sedimentary DNA? Toward the Reconstruction of Past Protistan Diversity, Microb. Ecol., 70, 865–875, https://doi.org/10.1007/s00248-015-0627-2, 2015.

Chiaia-Hernández, A. C., Günthardt, B. F., Frey, M. P., and Hollender, J.: Unravelling contaminants in the anthropocene using statistical analysis of liquid chromatography−high-resolution mass spectrometry nontarget screening data recorded in lake sediments, Environ. Sci. Technol., 51, 12547–12556, https://doi.org/10.1021/acs.est.7b03357, 2017.

Cvetkoska, A., Jovanovska, E., Hauffe, T., Donders, T. H., Levkov, Z., van de Waal, D. B., Reed, J. M., Francke, A., Vogel, H., Wilke, T., Wagner, B., and Wagner-Cremer, F.: Drivers of phytoplankton community structure change with ecosystem ontogeny during the Quaternary, Quat. Sci. Rev., 265, https://doi.org/10.1016/j.quascirev.2021.107046, 2021.

Dale, B., and Fjellså, A.: Dinoflagellate Cysts as Paleoproductivity Indicators: State of the Art, Potential, and Limits, in: Carbon Cycling in the Glacial Ocean: Constraints on the Ocean's Role in Global Change, NATO ASI Series, edited by: Zahn, R., Pedersen, T. F., Kaminski, M. A., Labeyrie, L., Springer, Berlin, Heidelberg, Germany, 521–537, https://doi.org/10.1007/978-3-642-78737-9_22, 1994.

De Vries, A., and Ripley, B. D.: ggdendro: Create Dendrograms and Tree Diagrams Using 'ggplot2', R package version 0.2.0, 2024.

Deng, K. K., Li, Y. X., Yan, P., Huo, Y. C., Yang, H., Chen, B., He, Q., Lin, G. J., and Guo, J. S.: Different preferences for inorganic carbon influence CO2 flux under Cyanobacteria or Chlorophyta dominance days, J. Environ. Manag., 370, https://doi.org/10.1016/j.jenvman.2024.122662, 2024.

Dittrich, M., Wehrli, B., and Reichert, P.: Lake sediments during the transient eutrophication period: Reactive-transport model and identifiability study, Ecol. Modell., 220, 2751–2769, https://doi.org/10.1016/j.ecolmodel.2009.07.015, 2009.

Elliott, J. A., Thackeray, S. J., Huntingford, C., and Jones, R. G.: Combining a regional climate model with a phytoplankton community model to predict future changes in phytoplankton in lakes, Freshw. Biol. 50, 1404–1411, https://doi.org/10.1111/j.1365-2427.2005.01409.x, 2005.

Elvert, M. and Niemann, H.: Occurrence of unusual steroids and hopanoids derived from aerobic methanotrophs at an active marine mud volcano, Org. Geochem., 39, 167–177, https://doi.org/10.1016/j.orggeochem.2007.11.006, 2008.

Epp, L. S., Zimmermann, H. H., Stoof-Leichsenring, K. R.: Sampling and Extraction of Ancient DNA from Sediments, in: Ancient DNA: Methods and Protocols, Methods in Molecular Biology, 1963, edited by: Shapiro, B., Barlow, A., Heintzman, P., Hofreiter, M., Paijmans, J., Soares, A., Humana Press, New York, USA, https://doi.org/10.1007/978-1-4939-9176-1_5, 2019.

Farrington, J. W. and Quinn, J. G.: "Unresolved Complex Mixture" (UCM): A brief history of the term and moving beyond it, Mar. Pollut. Bull., 96, 29–31, https://doi.org/10.1016/j.marpolbul.2015.04.039, 2015.

Furrer, O. J., and Gächter, R.: Der Beitrag der Landwirtschaft zur Eutrophierung der Gewässer in der Schweiz, Schweizerische Zeitschrift für Hydrologie, 34, 71–93, 1972.

https://doi.org/10.5194/egusphere-2026-4300
Preprint. Discussion started: 24 August 2026

Gfeller, V., Waelchli, J., Pfister, S., Deslandes-Hérold, G., Mascher, F., Glauser, G., Aeby, Y., Mestrot, A., Robert, C. A. M., Schlaeppi, K., and Erb, M.: Plant secondary metabolite-dependent plant-soil feedbacks can improve crop yield in the field, Elife, 12, https://doi.org/10.7554/eLife.84988, 2023.

Goad, J. L., and Akihisa. T.: Mass spectrometry of sterols, in: Analysis of Sterols, Springer, Dordrecht, Netherlands, https://doi.org/10.1007/978-94-009-1447-6_7, 1997.

Gray, J. R., Lacrampe-Couloume, G., Gandhi, D., Scow, K. M., Wilson, R. D., Mackay, D. M., and Sherwood Lollar, B.: Carbon and hydrogen isotopic fractionation during biodegradation of methyl tert-butyl ether, Environ. Sci. Technol., 36, 1931–1938, https://doi.org/10.1021/es011135n, 2002.

Hedberg, P., Albert, S., Nascimento, F. J. A., and Winder, M.: Effects of changing phytoplankton species composition on carbon and nitrogen uptake in benthic invertebrates, Limnol. Oceanogr., 66, 469–480, https://doi.org/10.1002/lno.11617, 2021.

Heinzelmann, S. M., Villanueva, L., Sinke-Schoen, D., Sinninghe Damsté, J. S., Schouten, S., and van der Meer, M. T. J.: Impact of metabolism and growth phase on the hydrogen isotopic composition of microbial fatty acids, Front. Microbiol., 6, https://doi.org/10.3389/fmicb.2015.00408, 2015.

Hinder, S. L., Hays, G. C., Edwards, M., Roberts, E. C., Walne, A. W., and Gravenor, M. B.: Changes in marine dinoflagellate and diatom abundance under climate change, Nat. Clim. Chang., 2, 271–275, https://doi.org/10.1038/nclimate1388, 2012.

Hirave, P., Glendell, M., Birkholz, A., and Alewell, C.: Compound-specific isotope analysis with nested sampling approach detects spatial and temporal variability in the sources of suspended sediments in a Scottish mesoscale catchment, Sci. Tot. Environ., 755, https://doi.org/10.1016/j.scitotenv.2020.142916, 2021.

Hollander, D. J. Mckenzie, J. A., and ten Haven, H. L: A 200 year sedimentary record of progressive eutrophication in Lake Greifen (Switzerland): Implications for the origin of organic-carbon-rich sediments, Geology 20, 825-828. https://doi.org/10.1130/0091-7613(1992)020<0825:AYSROP>2.3.CO;2, 1992.

Hou, W., Dong, H., Li, G., Yang, J., Coolen, M. J. L., Liu, X., Wang, S., Jiang, H., Wu, X., Xiao, H., Lian, B., and Wan, Y.: Identification of photosynthetic plankton communities using sedimentary ancient DNA and their response to late-holocene climate change on the Tibetan Plateau, Sci. Rep., 4, https://doi.org/10.1038/srep06648, 2014.

Huisman, J., Codd, G. A., Paerl, H. W., Ibelings, B. W., Verspagen, J. M. H., and Visser, P. M.: Cyanobacterial blooms, https://doi.org/10.1038/s41579-018-0040-1, Nat. Rev. Microbiol. 16, 471–483, 2018.

Huntscha, S., Stravs, M. A., Bühlmann, A., Ahrens, C. H., Frey, J. E., Pomati, F., Hollender, J., Buerge, I. J., Balmer, M. E., and Poiger, T.: Seasonal Dynamics of Glyphosate and AMPA in Lake Greifensee: Rapid Microbial Degradation in the Epilimnion during Summer, Environ. Sci. Technol., 52, 4641–4649, https://doi.org/10.1021/acs.est.8b00314, 2018.

Juggins, S.: rioja: Analysis of Quaternary Science Data, R package version (1.0-7), 2024.

Kawamura, K., Ishiwatari, R., and Oguka, K.: Early diagenesis of organic matter in the water column and sediments: Microbial degradation and resynthesis of lipids in Lake Haruna, Org. Geochem, 251–264, 1987.

https://doi.org/10.5194/egusphere-2026-4300
Preprint. Discussion started: 24 August 2026

Killops, S., and Killops, V.: Chemical Stratigraphic Concepts and Tools, in: Introduction to Organic Geochemistry, Blackwell publishing company, Oxford, UK, 166-245, 2004.

King, L., Devey, M., Leavitt, P. R., Power, M. J., Brothers, S., and Brahney, J.: Anthropogenic forcing leads to an abrupt shift to phytoplankton dominance in a shallow eutrophic lake, Freshw. Biol., 69, 335–350, https://doi.org/10.1111/fwb.14214, 2024.

Klatt, A., de Jonge, C., Nelson, D. B., Reyes, M., Schubert, C. J., Dubois, N., and Ladd, S. N.: Algal lipid distributions and hydrogen isotope ratios reflect phytoplankton community dynamics, Geochim. Cosmochim. Acta, 394, 205–219, https://doi.org/10.1016/j.gca.2025.02.013, 2025.

Kuhn, M. (2008). Building Predictive Models in R Using the caret Package. J. Stat. Softw. 28(5), 1–26. https://doi.org/10.18637/jss.v028.i05

Ladd, S. N., Nelson, D. B., Matthews, B., Dyer, S., Limberger, R., Klatt, A., Narwani, A., Dubois, N., and Schubert, C. J.: Taxon-specific hydrogen isotope signals in cultures and mesocosms facilitate ecosystem and hydroclimate reconstruction, Geochim. Cosmochim. Acta, 390, 199–210, https://doi.org/10.1016/j.gca.2024.12.002, 2025.

Ladd, S. N., Nelson, D. B., Schubert, C. J., and Dubois, N.: Lipid compound classes display diverging hydrogen isotope responses in lakes along a nutrient gradient. Geochim. Cosmochim. Acta 237, 103–119, https://doi.org/10.1016/j.gca.2018.06.005, 2018.

Lampert, W., and Sommer, U.: Limnoökologie, Georg Thieme Verlag Stuttgart, 1993.

Lin, Q., Zhang, K., McGowan, S., Capo, E., and Shen, J.: Synergistic impacts of nutrient enrichment and climate change on long-term water quality and ecological dynamics in contrasting shallow-lake zones, Limnol. Oceanogr., 66, 3271–3286, https://doi.org/10.1002/lno.11878, 2021.

Liu, X., Sun, J., Wei, Y., and Liu, Y.: Relationship between cell volume and particulate organic matter for different size phytoplankton, Mar. Pollut. Bull., 194, https://doi.org/10.1016/j.marpolbul.2023.115298, 2023.

Lotter, A. F.: Paläoökologische und paläolimnologische Studie des Rotsees bei Luzern, in: Dissertationes Botanicae, 124, Schweizerbart Science Publishers, Stuttgart, Germany, 1988.

Lotter, A. F.: Subfossil and modern diatom plankton and the paleolimnology of Rotsee (Switzerland) since 1850, Aquat. Sci., 51, 338–350, https://doi.org/10.1007/BF00877176, 1989.

Lotter, A. F.: The effect of eutrophication on diatom diversity: examples from six Swiss lakes, in: Lange-Bertalot-Festschrift: Studies on Diatoms, edited by: Jahn, R., J.P. Kociolek, A. Witkowski and P. Compere, Gantner, Ruggell, Berlin, Germany, 417–432, 2001.

M'Boule, D., Chivall, D., Sinke-Schoen, D., Sinninghe Damsté, J. S., Schouten, S., and van der Meer, M. T. J.: Salinity dependent hydrogen isotope fractionation in alkenones produced by coastal and open ocean haptophyte algae, Geochim. Cosmochim. Acta, 130, 126–135. https://doi.org/10.1016/j.gca.2014.01.029, 2014.

Maerki, M., Müller, B., Dinkel, C., and Wehrli, B.: Mineralization pathways in lake sediments with different oxygen and organic carbon supply, Limnol. Oceanogr., 54, 428–438, https://doi.org/10.4319/lo.2009.54.2.0428, 2009.

https://doi.org/10.5194/egusphere-2026-4300
Preprint. Discussion started: 24 August 2026

Makri, S., Lami, A., Lods-Crozet, B., and Loizeau, J. L.: Reconstruction of trophic state shifts over the past 90 years in a eutrophicated lake in western Switzerland, inferred from the sedimentary record of photosynthetic pigments, J. Paleolimnol., 61, 129–145, https://doi.org/10.1007/s10933-018-0049-5, 2019.

Martin-Creuzburg, D., von Elert, E., and Hoffmann, K. H.: Nutritional constraints at the cyanobacteria-Daphnia magna interface: The role of sterols, Limnol. Oceanogr., 53, 456–468, https://doi.org/10.4319/lo.2008.53.2.0456, 2008.

Mattern, J. P., Glauninger, K., Britten, G. L., Casey, J. R., Hyun, S., Wu, Z., Armbrust, E. V., Harchaoui, Z., and Ribalet, F.: A Bayesian approach to modeling phytoplankton population dynamics from size distribution time series, PLoS Comput. Biol., 18, https://doi.org/10.1371/journal.pcbi.1009733, 2022.

Merz, E., Saberski, E., Gilarranz, L. J., Isles, P. D. F., Sugihara, G., Berger, C., and Pomati, F.: Disruption of ecological networks in lakes by climate change and nutrient fluctuations, Nat. Clim. Chang., 13, 389–396, https://doi.org/10.1038/s41558-023-01615-6, 2023.

Meyers, P. A. and Ishiwatari, R.: Lacustrine organic geochemistryman overview of indicators of organic matter sources and diagenesis in lake sediments, Org. Geochem, 867–900, 1993.

Mieleitner, J., and Reichert, P.: Modelling functional groups of phytoplankton in three lakes of different trophic state, Ecol. Modell. 211, 279–291. https://doi.org/10.1016/j.ecolmodel.2007.09.010, 2008.

Montassier, E., Al-Ghalith, G. A., Hillmann, B., Viskocil, K., Kabage, A. J., McKinlay, C. E., Sadowsky, M. J., Khoruts, A., and Knights, D.: CLOUD: A non-parametric detection test for microbiome outliers, Microbiome, 6, https://doi.org/10.1186/s40168-018-0514-4, 2018.

Naeher, S., Smittenberg, R. H., Gilli, A., Kirilova, E. P., Lotter, A. F., and Schubert, C. J.: Impact of recent lake eutrophication on microbial community changes as revealed by high resolution lipid biomarkers in Rotsee (Switzerland), Org. Geochem., 49, 86–95, https://doi.org/10.1016/j.orggeochem.2012.05.014, 2012.

Naeher, S., Suga, H., Ogawa, N. O., Schubert, C. J., Grice, K., and Ohkouchi, N.: Compound-specific carbon and nitrogen isotopic compositions of chlorophyll a and its derivatives reveal the eutrophication history of Lake Zurich (Switzerland), Chem. Geol., 443, 210–219, https://doi.org/10.1016/j.chemgeo.2016.09.005, 2016.

Narwani, A., Reyes, M., Pereira, A.L., Penson, H., Dennis, S.R., Derrer, S., Spaak, P., Matthews, B.: Interactive effects of foundation species on ecosystem functioning and stability in response to disturbance, Proc R Soc B: Biol. Sci, 286, 20191857, https://doi.org/10.1098/rspb.2019.1857, 2019.

Nelson, D. B. and Sachs, J. P.: The influence of salinity on D/H fractionation in dinosterol and brassicasterol from globally distributed saline and hypersaline lakes, Geochim. Cosmochim. Acta, 133, 325–339, https://doi.org/10.1016/j.gca.2014.03.007, 2014.

Nürnberg, G. K.: Importance of considering internal phosphorus loading during climate change in predicting and managing cyanobacteria, Lake Reserv. Manag., 41, 165–179, https://doi.org/10.1080/10402381.2025.2538244, 2025.

Nwosu, E. C., Brauer, A., Monchamp, M. E., Pinkerneil, S., Bartholomäus, A., Theuerkauf, M., Schmidt, J. P., Stoof-Leichsenring, K. R., Wietelmann, T., Kaiser, J., Wagner, D., and Liebner, S.: Early human impact on lake cyanobacteria

https://doi.org/10.5194/egusphere-2026-4300
Preprint. Discussion started: 24 August 2026

revealed by a Holocene record of sedimentary ancient DNA, Commun. Biol., 6, https://doi.org/10.1038/s42003-023-04430-z, 2023.

Oksanen, J., Simpson, G,., Blanchet, F., Kindt, R., Legendre, P., Minchin, P., O'Hara, R.B., Solymos, P., Stevens, M.H.H., Szoecs, E., Wagner, H., Barbour, M., Bedward, M., Bolker, B., Borcard, D., Carvalho, G., Chirico, M., De Caceres, M., Durand, S., Evangelista, H.B.A., FitzJohn, R., Friendly, M., Furneaux, B., Hannigan, G., Hill, M.O., Lahti, L., McGlinn, D., Ouellette, M.-H., Cunha, E.R., Smith, T., Stier, A., Ter Braak, C.J.F., Weedon, J.: vegan: Community Ecology Package, R package version 2.7-2, 2025.

Ourisson, G., Rohmer, M., and Poralla, K.: Prokaryotic Hopanoids and other Polyterpenoid Sterol Surrogates, Ann. Rev. Microbiol., 41, 301-333, https://doi.org/10.1146/annurev.mi.41.100187.001505, 1987.

Pandolfini, E., Thys, I., Leporcq, B., and Descy, J.-P.: Grazing experiments with two freshwater zooplankters: fate of chlorophyll and carotenoid pigments, J. Plankton Res. 22, 305–319, https://doi.org/10.1093/plankt/22.2.305, 2000.

Pearce, G. E. S., Harradine, P. J., Talbot, H. M., and Maxwell, J. R.: Sedimentary sterols and steryl chlorin esters: distribution differences and signifcance, Org. Geochem., 28, 3-10, 1998.

Peltomaa, E., Asikainen, H., Blomster, J., Pakkanen, H., Rigaud, C., Salmi, P., and Taipale, S.: Phytoplankton group identification with chemotaxonomic biomarkers: In combination they do better, Phytochemistry, 209, https://doi.org/10.1016/j.phytochem.2023.113624, 2023.

Perry, G. J., Volkman, J. K., Johns, R. B., and Bavor Jr H. J.: Fatty acids of bacterial origin in contemporary marine sediments, Geochim. Cosmochim. Acta, 43, 1715-1725, 1979.

Pilecky, M., Kainz, M.J., and Wassenaar, L.I.: Exploring hydrogen isotope fractionation in lipid biomolecules of freshwater algae: implications for ecological and paleoenvironmental studies, Isot. Environ. Health Stud., 60, 585–595, 2024.

Podani, J. and Miklós, I.: Resemblance Coefficients and the Horseshoe Effect in Principal Coordinates Analysis, Ecology 83, 3331–3343, https://doi.org/10.2307/3072083, 2002.

Prahl, F. G., Eglinton, G., Corner, E. D. S., O'Hara, S. C. M., and Forsberg, T. E. V.: Changes in plant lipids during passage through the gut of calanus, J. Mar. Biol. Assoc. U. K., 64, 317–334, https://doi.org/10.1017/S0025315400030022, 1984.

Reuss, N., Conley, D. J., and Bianchi, T. S.: Preservation conditions and the use of sediment pigments as a tool for recent ecological reconstruction in four Northern European estuaries, Mar. Chem., 95, 283–302, https://doi.org/10.1016/j.marchem.2004.10.002, 2005.

Rivier, O.: Recherche hydrobiologique sur le Lac de Morat, Extrait du Bulletin de la Société neuchâteloise des Sciences naturelles, 61, 1936.

https://doi.org/10.5194/egusphere-2026-4300
Preprint. Discussion started: 24 August 2026

Romahn, J., Schmidt, A., Kaiser, J., Baranski, D., Arz, H. W., Epp, L. S., Kremp, A., and Bálint, M.: Extending monitoring with sediment archive approaches: Comparison of biomonitoring, metabarcoding, and biomarkers to assess past phytoplankton dynamics, Limnol. Oceanogr. Methods, 23, 578–593, https://doi.org/10.1002/lom3.10694, 2025.

Rustan, A. C. and Drevon, C. A.: Fatty Acids: Structures and Properties, Encyclopedia of Life Sciences, https://doi.org/10.1038/npg.els.0003894, 2005.

Sachs, J. P. and Schwab, V. F.: Hydrogen isotopes in dinosterol from the Chesapeake Bay estuary, Geochim. Cosmochim. Acta, 75, 444–459, https://doi.org/10.1016/j.gca.2010.10.013, 2011.

Schouten, S., Ossebaar, J., Schreiber, K., Kienhuis, M.V.M., Langer, G., Benthien, A., and Bijma, J.: The effect of temperature, salinity and growth rate on the stable hydrogen isotopic composition of long chain alkenones produced by *Emiliania huxleyi* and *Gephyrocapsa oceanica*. Biogeosciences 3, 113–119, 2006.

Schouten, S. J., Schmidhauser, N. R. M. M., Grosjean, M., Lami, A., Boltshauser-Kaltenrieder, P., van Leeuwen, J. F. N., Vogel, H., and Zahajská, P.: Lake anoxia, primary production and algal community shifts in response to rapid climate changes during the Late-Glacial, Biogeosciences, 22, 3821–3842, 2025 https://doi.org/10.5194/bg-22-3821-2025, 2025.

Schubert, C.J., Villanueva, J., Calvert, S.E., Cowie, G.L., von Rad, U., Schulz, H., Berner, U., and Erlenkeuser, H.: Stable phytoplankton community structure in the Arabian Sea over the past 200,000 years, *Nature* 394, 563–566, https://doi.org/10.1038/29047, 1998.

Sheath, R. G. and Wehr, J. D.: Introduction to the Freshwater Algae, in: Freshwater Algae of North America: Ecology and Classification, Elsevier Inc., 1–11, https://doi.org/10.1016/B978-0-12-385876-4.00001-3, 2015.

Shen, J., Pearson, A., Henkes, G. A., Zhang, Y. G., Chen, K., Li, D., Wankel, S. D., Finney, S. C., and Shen, Y.: Improved efficiency of the biological pump as a trigger for the Late Ordovician glaciation, Nat. Geosci., 11, 510–514, https://doi.org/10.1038/s41561-018-0141-5, 2018.

Sherwood, A. R. and Presting, G. G.: Universal primers amplify a 23S rDNA plastid marker in eukaryotic algae and cyanobacteria, J. Phycol., 43, 605–608, https://doi.org/10.1111/j.1529-8817.2007.00341.x, 2007.

Soracreppa, B.: Jahreszeitliche Veränderungen von Wasserchemismus und Phykozönosen in zehn Seen der Umgebung von Zürich, Vierteljahrsschr. Naturforsch. Ges. Zürich, 123, 161-235, 1978.

Steenbergen, C. L. M., Korthals, H. J., and Dobrynin, E. G.: Algal and bacterial pigments in non-laminated lacustrine sediment: Studies of their sedimentation, degradation and stratigraphy, FEMS Microbiol. Ecol., 13, 335-352, 1994.

Steven, B., Mccann, S., and Ward, N. L.: Pyrosequencing of plastid 23S rRNA genes reveals diverse and dynamic cyanobacterial and algal populations in two eutrophic lakes, FEMS Microbiol. Ecol., 82, 607–615, https://doi.org/10.1111/j.1574-6941.2012.01429.x, 2012.

Strassmann, K. M., Brennwald, M. S., Peeters, F., and Kipfer, R.: Dissolved noble gases in the porewater of lacustrine sediments as palaeolimnological proxies, Geochim. Cosmochim. Acta, 69, 1665–1674, https://doi.org/10.1016/j.gca.2004.07.037, 2005.

https://doi.org/10.5194/egusphere-2026-4300
Preprint. Discussion started: 24 August 2026

Taipale, S., Strandberg, U., Peltomaa, E., Galloway, A. W. E., Ojala, A., and Brett, M. T.: Fatty acid composition as biomarkers of freshwater microalgae: Analysis of 37 strains of microalgae in 22 genera and in seven classes, Aquat. Microb. Ecol., 71, 165–178, https://doi.org/10.3354/ame01671, 2013.

Taipale, S. J., Hiltunen, M., Vuorio, K., and Peltomaa, E.: Suitability of phytosterols alongside fatty acids as chemotaxonomic biomarkers for phytoplankton, Front. Plant Sci., 7, https://doi.org/10.3389/fpls.2016.00212, 2016.

Takasu, H., Ushio, M., LeClair, J. E., and Nakano, S. I.: High contribution of Synechococcus to phytoplankton biomass in the aphotic hypolimnion in a deep freshwater lake (Lake Biwa, Japan), Aquat. Microb. Ecol., 75, 69–79, https://doi.org/10.3354/ame01749, 2015.

Tang, L., Tam, N. F.-Y., Lam, W., Lee, T. C.-H., Xu, S. J.-L., Lee, C.-L., and Lee, F. W.-F.: Interpreting the complexities of the plastid genome in dinoflagellates: a mini-review of recent advances, Plant Mol. Biol., 114, 2024.

Taranu, Z. E., Gregory-Eaves, I., Leavitt, P. R., Bunting, L., Buchaca, T., Catalan, J., Domaizon, I., Guilizzoni, P., Lami, A., Mcgowan, S., Moorhouse, H., Morabito, G., Pick, F. R., Stevenson, M. A., Thompson, P. L., and Vinebrooke, R. D.: Acceleration of cyanobacterial dominance in north temperate-subarctic lakes during the Anthropocene, Ecol. Lett., 18, 375–384, https://doi.org/10.1111/ele.12420, 2015.

Thomas, E. A.: Rotalgenrasen und Blaualgenteppiche im Zürichsee, Vierteljahrsschr. Naturforsch. Ges. Zürich, 105, 297-305, 1960.

Thorpe, A. C., Mackay, E. B., Goodall, T., Bendle, J. A., Thackeray, S. J., Maberly, S. C., and Read, D. S.: Evaluating the use of lake sedimentary DNA in palaeolimnology: A comparison with long-term microscopy-based monitoring of the phytoplankton community, Mol. Ecol. Resour., 24, https://doi.org/10.1111/1755-0998.13903, 2024.

Tortell, P. D.: Evolutionary and ecological perspectives on carbon acquisition in phytoplankton, Limnol. Oceanogr., 45, 744–750, https://doi.org/10.4319/lo.2000.45.3.0744, 2000.

Venkatesan, M. I.: Tetrahymanol: Its widespread occurrence and geochemical significance, Geochim. Cosmochim. Acta 53, 3095-3101, 1989.

Volkman, J. K.: Sterols in microorganisms, https://doi.org/10.1007/s00253-002-1172-8, 2003.

Volkman, J. K., Barrett, S. M., Dunstan, G. A., and Jeffrey, S. W.: Geochemical significance of the occurrence of dinosterol and other 4-methyl sterols in a marine diatom, Org. Geochem, 7–15, 1993.

Wang, L. G., Lam, T. T. Y., Xu, S., Dai, Z., Zhou, L., Feng, T., Guo, P., Dunn, C. W., Jones, B. R., Bradley, T., Zhu, H., Guan, Y., Jiang, Y., and Yu, G.: Treeio: An R Package for Phylogenetic Tree Input and Output with Richly Annotated and Associated Data, Mol. Biol. Evol., 37, 599–603, https://doi.org/10.1093/molbev/msz240, 2020.

Watanabe, S.: Cyanobacterial multi-copy chromosomes and their replication, Biosci. Biotechn. Biochem. 84, 1309–1321, https://doi.org/10.1080/09168451.2020.1736983, 2020.

https://doi.org/10.5194/egusphere-2026-4300
Preprint. Discussion started: 24 August 2026

Weber, J., Bauersachs, T., and Schwark, L.: A multiphasic Younger Dryas cold period recorded in sediments of Lake Steisslingen, SW-Germany: A biomarker perspective, Quat. Int., 542, 121–136, https://doi.org/10.1016/j.quaint.2020.03.028, 2020.

Weiss, S., Xu, Z. Z., Peddada, S., Amir, A., Bittinger, K., Gonzalez, A., Lozupone, C., Zaneveld, J. R., Vázquez-Baeza, Y., Birmingham, A., Hyde, E. R., and Knight, R.: Normalization and microbial differential abundance strategies depend upon data characteristics, Microbiome, 5, https://doi.org/10.1186/s40168-017-0237-y, 2017.

Wickham, H.: ggplot2: Elegant Graphics for Data Analysis, Springer, New York, USA, 2009.

Wijker, R. S., Sessions, A. L., Fuhrer, T., and Phan, M.: 2H/1H variation in microbial lipids is controlled by NADPH metabolism, PNAS, 116, 12173–12182, https://doi.org/10.1073/pnas.1818372116, 2019.

Wilke, C.: cowplot: Streamlined Plot Theme and Plot Annotations for 'ggplot2', R package version 1.2.0, 2025.

Witkowski, C. R., van der Meer, M. T. J., Blais, B., Sinninghe Damsté, J. S., and Schouten, S.: Algal biomarkers as a proxy for pCO2: Constraints from late quaternary sapropels in the eastern Mediterranean, Org. Geochem., 150, https://doi.org/10.1016/j.orggeochem.2020.104123, 2020.

Xu, S., Dai, Z., Guo, P., Fu, X., Liu, S., Zhou, L., Tang, W., Feng, T., Chen, M., Zhan, L., Wu, T., Hu, E., Jiang, Y., Bo, X., and Yu, G.: GgtreeExtra: Compact Visualization of Richly Annotated Phylogenetic Data, Mol Biol Evol, 38, 4039–4042, https://doi.org/10.1093/molbev/msab166, 2021.

Xu, S., Li, L., Luo, X., Chen, M., Tang, W., Zhan, L., Dai, Z., Lam, T., Guan, Y., Yu, G.: Ggtree: A serialized data object for visualization of a phylogenetic tree and annotation data, iMeta, 4, e56, 2022.

Xu, S., Li, G., He, C., Huang, Y., Yu, D., Deng, H., Tong, Z., Wang, Y., Dupuy, C., Huang, B., Shen, Z., Xu, J., and Gong, J.: Diversity, community structure, and quantity of eukaryotic phytoplankton revealed using 18S rRNA and plastid 16S rRNA genes and pigment markers: a case study of the Pearl River Estuary, Mar. Life Sci. Technol., 5, 415–430, https://doi.org/10.1007/s42995-023-00186-x, 2023.

Yan, D., Picard, M., Han, Y., An, Z., Lei, D., Zhao, X., Zhang, L., and Capo, E.: Sedimentary DNA reveals phytoplankton diversity loss in a deep maar lake during the Anthropocene, Limnol. Oceanogr., 69, 1299–1315, https://doi.org/10.1002/lno.12562, 2024.

Yan, X., Xia, Y., Ti, C., Shan, J., Wu, Y., and Yan, X.: Thirty years of experience in water pollution control in Taihu Lake: A review, Sci. Total Environ., 914, https://doi.org/10.1016/j.scitotenv.2023.169821, 2024.

Yu, G.: Using ggtree to visualize data on tree-like structures. Current Protocols in Bioinformatics, 69, e96, 2020.

Yu, G., Smith, D. K., Zhu, H., Guan, Y., and Lam, T. T. Y.: ggtree: an r package for visualization and annotation of phylogenetic trees with their covariates and other associated data, Methods Ecol. Evol. 8(1), 28–36. https://doi.org/10.1111/2041-210X.12628, 2017.

Yu, G., Lam, T. T., Zhu, H., Guan, Y.: Two methods for mapping and visualizing associated data on phylogeny using ggtree, Mol. Biol. Evolut. 35, 3041-3043, 2018.

https://doi.org/10.5194/egusphere-2026-4300
Preprint. Discussion started: 24 August 2026

Zhang, X., Gillespie, A. L., and Sessions, A. L.: Large D/H variations in bacterial lipids reflect central metabolic pathways, PNAS, 12580–12586, 2009.

Zhang, Y., Peng, T., Yu, J., Su, Y., and Liu, Z.: Natural and anthropogenically driven changes in the n-alkanols of lake sediments and implications for their use in paleoenvironmental studies of lakes, Catena (Amst), 207, https://doi.org/10.1016/j.catena.2021.105591, 2021.

Zhang, Z., Green, B. R., and Cavalier-Smith, T.: Single gene circles in dinoflagellate chloroplast genomes, Nature 400, 155–159, https://doi.org/10.1038/22099, 1999.

Zhang, Z., Green, B. R., and Cavalier-Smith, T.: Phylogeny of ultra-rapidly evolving dinoflagellate chloroplast genes: A possible common origin for sporozoan and dinoflagellate plastids, J. Mol. Evol., 51, 26–40, https://doi.org/10.1007/s002390010064, 2000.

Zhang, Z., and Sachs, J. P.: Hydrogen isotope fractionation in freshwater algae: I. Variations among lipids and species, Org. Geochem. 38, 582–608. https://doi.org/10.1016/j.orggeochem.2006.12.004, 2007.